NASA/TM–2015-218772

Multi-Level Experimental and Analytical Evaluation of Two Composite Energy Absorbers

Karen E. Jackson and Justin D. Littell
Langley Research Center, Hampton, Virginia

Edwin L. Fasanella
National Institute of Aerospace, Hampton, Virginia

Martin S. Annett
Langley Research Center, Hampton, Virginia

Michael D. Seal, II
Analytical Mechanics Associates, Inc., Hampton, Virginia

July 2015

NASA STI Program . . . in Profile

Since its founding, NASA has been dedicated to the advancement of aeronautics and space science. The NASA scientific and technical information (STI) program plays a key part in helping NASA maintain this important role.

The NASA STI program operates under the auspices of the Agency Chief Information Officer. It collects, organizes, provides for archiving, and disseminates NASA's STI. The NASA STI program provides access to the NTRS Registered and its public interface, the NASA Technical Reports Server, thus providing one of the largest collections of aeronautical and space science STI in the world. Results are published in both non-NASA channels and by NASA in the NASA STI Report Series, which includes the following report types:

- TECHNICAL PUBLICATION. Reports of completed research or a major significant phase of research that present the results of NASA Programs and include extensive data or theoretical analysis. Includes compilations of significant scientific and technical data and information deemed to be of continuing reference value. NASA counter-part of peer-reviewed formal professional papers but has less stringent limitations on manuscript length and extent of graphic presentations.

- TECHNICAL MEMORANDUM. Scientific and technical findings that are preliminary or of specialized interest, e.g., quick release reports, working papers, and bibliographies that contain minimal annotation. Does not contain extensive analysis.

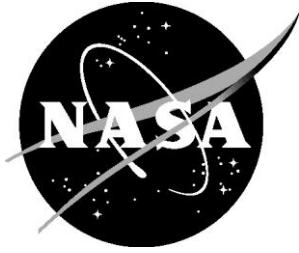- CONTRACTOR REPORT. Scientific and technical findings by NASA-sponsored contractors and grantees.

- CONFERENCE PUBLICATION. Collected papers from scientific and technical conferences, symposia, seminars, or other meetings sponsored or co-sponsored by NASA.

- SPECIAL PUBLICATION. Scientific, technical, or historical information from NASA programs, projects, and missions, often concerned with subjects having substantial public interest.

- TECHNICAL TRANSLATION. English-language translations of foreign scientific and technical material pertinent to NASA's mission.

Specialized services also include organizing and publishing research results, distributing specialized research announcements and feeds, providing information desk and personal search support, and enabling data exchange services.

For more information about the NASA STI program, see the following:

- Access the NASA STI program home page at http://www.sti.nasa.gov

- E-mail your question to help@sti.nasa.gov

- Phone the NASA STI Information Desk at 757-864-9658

- Write to:
  NASA STI Information Desk
  Mail Stop 148
  NASA Langley Research Center
  Hampton, VA 23681-2199

Multi-Level Experimental and Analytical Evaluation of Two Composite Energy Absorbers

Karen E. Jackson and Justin D. Littell
Langley Research Center, Hampton, Virginia

Edwin L. Fasanella
National Institute of Aerospace, Hampton, Virginia

Martin S. Annett
Langley Research Center, Hampton, Virginia

Michael D. Seal, II
Analytical Mechanics Associates, Inc., Hampton, Virginia

July 2015

Multi-Level Experimental and Analytical Evaluation of Two Composite Energy Absorbers

Karen E. Jackson
NASA Langley Research Center

Justin D. Littell
NASA Langley Research Center

Edwin L. Fasanella
National Institute of Aerospace

Martin S. Annett
NASA Langley Research Center

Michael D. Seal
Analytical Mechanics Associates, Inc.

Mail Stop 495
NASA Langley Research Center
Hampton, VA 23681

1.0 ABSTRACT

Two composite energy absorbers were developed and evaluated at NASA Langley Research Center through multi-level testing and simulation performed under the Transport Rotorcraft Airframe Crash Testbed (TRACT) research program. A conical-shaped energy absorber, designated the conusoid, was evaluated that consisted of four layers of hybrid carbon-Kevlar[®] plain weave fabric oriented at [+45°/-45°/-45°/+45°] with respect to the vertical, or crush, direction. A sinusoidal-shaped energy absorber, designated the sinusoid, was developed that consisted of hybrid carbon-Kevlar[®] plain weave fabric face sheets, two layers for each face sheet oriented at ±45° with respect to the vertical direction and a closed-cell ELFOAM[®] P200 polyisocyanurate (2.0-lb/ft^3) foam core. The design goal for the energy absorbers was to achieve average floor-level accelerations of between 25- and 40-g during the full-scale crash test of a retrofitted CH-46E helicopter airframe, designated TRACT 2. Variations in both designs were assessed through dynamic crush testing of component specimens. Once the designs were finalized, subfloor beams of each configuration were fabricated and retrofitted into a barrel section of a CH-46E helicopter. A vertical drop test of the barrel section was conducted onto concrete to evaluate the performance of the energy absorbers prior to retrofit into TRACT 2. The retrofitted airframe was crash tested under combined forward and vertical velocity conditions onto soil, which is characterized as a sand/clay mixture. Finite element models were developed of all test articles and simulations were performed using LS-DYNA[®], a commercial nonlinear explicit transient dynamic finite element code. Test-analysis results are presented for each energy absorber as comparisons of time-history responses, as well as predicted and experimental structural deformations and progressive damage under impact loading for each evaluation level.

2.0 INTRODUCTION

In 2012, the NASA Rotary Wing (RW) Crashworthiness Program [1] initiated the Transport Rotorcraft Airframe Crash Testbed (TRACT) research program by obtaining two CH-46E helicopter airframes from the Navy CH-46E Program Office (PMA-226) at the Navy Flight Readiness Center in Cherry Point, North Carolina. Full-scale crash tests were planned to assess dynamic responses of transport-category rotorcraft under combined forward and vertical impact loading. The first crash test, TRACT 1 [2], was performed at NASA Langley Research Center's Landing and Impact Research Facility (LandIR). Impact tests conducted at LandIR provide data that enable the study of critical interactions between the airframe, seat, and occupant during a controlled crash environment. The CH-46E airframe is categorized as a medium-lift rotorcraft with length and width of 45- and 7-ft, respectively, and a capacity for 5 crew and 25 troops. TRACT 1 was

conducted in August 2013 under combined conditions of 300-in/s (25-ft/s) vertical and 396-in/s (33-ft/s) forward velocity onto soil, which is characterized as a sand/clay mixture. The primary objectives for TRACT 1 were to assess improvements in occupant loads and flail envelope with the use of crashworthy features such as pre-tensioning active restraints and energy absorbing seats and to develop novel techniques for photogrammetric data acquisition to measure occupant and airframe kinematics. Pre- and post-test photographs of the TRACT 1 crash test are shown in Figure 1.

(a) Pre-test photograph.   (b) Post-test photograph.
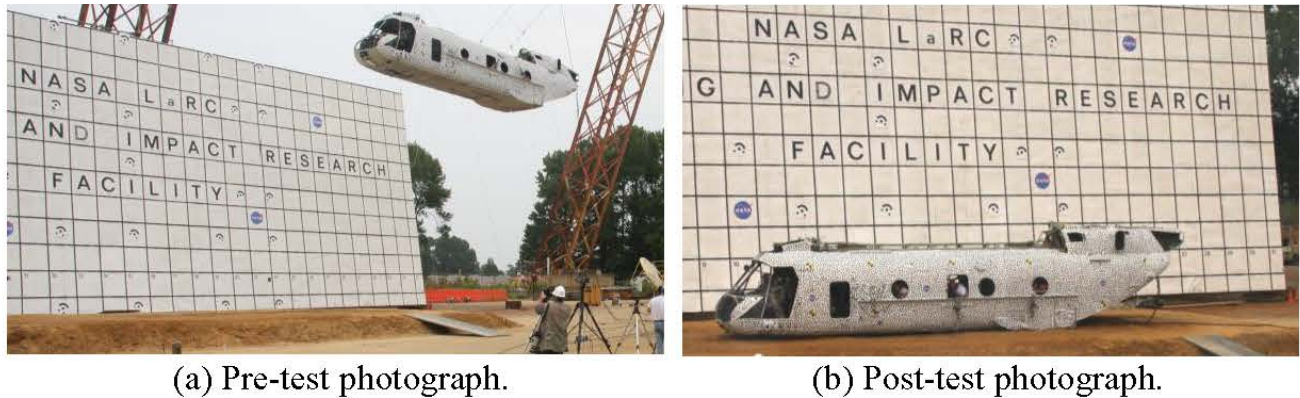
Figure 1. Pre- and post-test photographs of the TRACT 1 full-scale crash test.

The TRACT 1 airframe was tested in a baseline configuration with no changes to the structural configuration, including the discrete aluminum shear panels in the subfloor. It is important to note that the CH-46E does not contain a center keel beam; hence the airframe relies on the aluminum shear panels, the cargo rails in the floor, and the airframe structure to provide longitudinal and torsional stiffness. A final objective of TRACT 1 was to generate crash test data in a baseline configuration for comparison with data obtained from a similar TRACT 2 crash test. The crash test of the second CH-46E airframe (TRACT 2) was conducted on October 1, 2014 and was performed for the same nominal impact velocity conditions and onto the same sand/clay surface [3]. The difference is that the TRACT 2 airframe was retrofitted with three different composite energy absorbing subfloor concepts located in the mid-cabin region: a corrugated web design [4, 5] fabricated of graphite fabric; a conical-shaped design, designated the "conusoid," fabricated of four layers of hybrid carbon-Kevlar® fabric [6]; and, a sinusoidal-shaped foam sandwich design, designated the "sinusoid," fabricated of the same hybrid fabric face sheets with a foam core. While the TRACT 2 airframe contained similar seat, occupant, and restraint experiments, one of the major goals of the test was to evaluate the performance of novel composite energy absorbing subfloor designs for improved crashworthiness.

This paper will summarize the development of the conusoid and sinusoid foam sandwich energy absorbing concepts. Multi-level evaluations of the energy absorbers are discussed including dynamic crush testing and simulation of component specimens, vertical drop testing and simulation of a retrofitted barrel section, and full-scale crash testing and simulation of the TRACT 2 retrofitted helicopter airframe. Finite element models were developed of all test articles and simulations were performed using LS-DYNA® [7, 8], a commercial explicit nonlinear, transient dynamic finite element code. Thus, a final objective of this research program is to evaluate the capabilities of LS-DYNA® in predicting the dynamic response and progressive failure behavior of composite energy absorbing airframe structures.

3.0 DESCRIPTION OF THE COMPOSITE ENERGY ABSORBERS

3.1 Design Goals for the Energy Absorbers

Following the TRACT 1 crash test, a research effort was initiated to develop two composite energy absorbers for retrofit into the TRACT 2 test article. The design goals were to limit the average vertical accelerations to 25- to 40-g on the floor, to minimize peak crush loads, and to generate relatively long crush stroke limits under dynamic loading conditions, typical of those experienced during the TRACT 1 full-scale crash test [2]. To further clarify the design goals, it is important to note that the loading conditions on the frames of the TRACT 1 full-scale crash test provided dynamic crush loads of approximately 2,500- to 4,000-lb. per linear foot, measured from one side of the floor to the other (a distance of 60-in. or 5-ft). These values are determined by multiplying the design acceleration levels (25- to 40-g) by the floor mass loading of 100-lb per linear foot. Note that the weight times the g-factor equals the force. The loading condition was based on seat and occupant loads that were recorded during the TRACT1 crash test. A schematic drawing is shown in Figure 2 illustrating design conditions for floor loading.
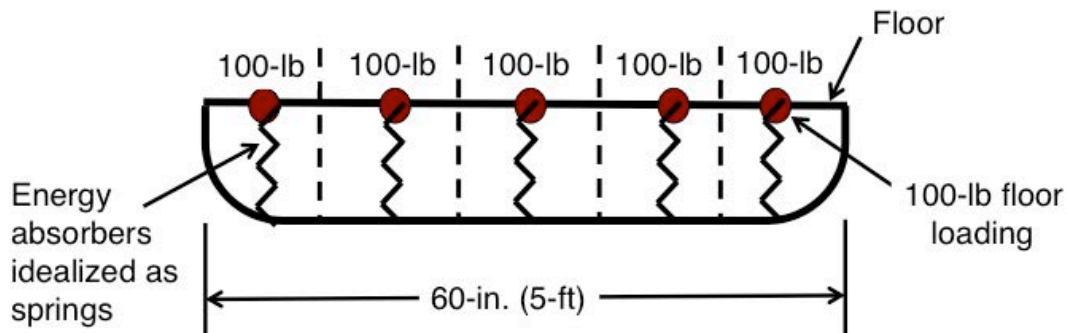

Figure 2. Floor loading condition schematic.

Figure 2 shows an idealized schematic of the floor and subfloor located at an individual fuselage frame. The floor, which is approximately 5-ft wide, is divided into 5 segments of 1-ft. length, each having an associated floor loading of 100-lb. The energy absorbers, depicted as individual springs, are designed to limit floor-level accelerations to 25- to 40-g.

Often, design goals for energy absorbers are defined in terms of Specific Sustained Crush Stress (SSCS). The SSCS is a measure of the energy absorbing capability of the material and is defined as

$$SSCS = P_{avg}/(A \times \rho) \hspace{3cm} Eq. 1$$

where P_{avg} is the average sustained crush load, A is the cross-sectional area, and ρ is the density of the material. The SSCS is also the energy absorbed per unit weight of material crushed. Assuming an average acceleration level of 25-g, a floor loading of 100 lb. for a 1-ft. length, a cross-sectional area of 0.98-in^2 and a material density of 0.03486-lb/in^3, an SSCS value of 72,590-in-lb/in is obtained for a typical conusoid energy absorber. This value is particularly high. For example, Reference 9 documents the energy absorption capabilities of flat plate composite specimens and reports values of SSCS ranging from 28,710- to 40,200-in-lb/in. Part of the explanation for the high SSCS value is the fact that an average crush load is based on the dynamic design goal. In Reference 6, the average crush load for the conusoid is reported between 900- to 1,500-lb, based on quasi-static loading. Using these averages, SSCS is lowered to values between 26,132- and 43,611-in-

3

lb/in. The SSCS is typically reported in metric units. Thus, a SSCS value of 72,590-in-lb/in is converted to 18.1-N m/g. Note that Farley [10] reported SSCS values of between 20- and 75-Nm/g for various composite tubes that were subjected to quasi-static compressive loads.

Farley [10, 11], Kindervater [12], Bannerman [13], and Hanagud [14] have investigated the crushing response of composite structural elements and sine wave beams. Farley [11] has shown that high values of SSCS are obtained when using hybrid graphite-Kevlar composites in which the graphite fibers are oriented in the same direction as the loading axis and the Kevlar fibers are oriented at 45° to the loading axis. As stated in Reference 11, "the Kevlar fibers are positioned in the laminate to provide containment and support for the graphite fibers, which absorb energy through a combination of crushing and fracturing modes."

3.2 Conusoid Energy Absorber

The first design is a novel conical sinusoid, or "conusoidal" composite energy absorber, also designated "conusoid." The geometry of the conusoid is based on alternating right-side-up and up-side down half-cones placed in a repeating pattern. The conusoid combines a simple cone design, which has been extensively studied in the literature [15-18], with sinusoidal beam geometry to create a structure that utilizes the advantages of both configurations. An isometric view of the conusoid is shown in Figure 3(a). Variations in geometry, materials, and laminate stacking sequences were evaluated during development of the conusoid and the final design consisted of four layers of a hybrid carbon-Kevlar® plain weave fabric oriented at [+45°/-45°/-45°/+45°] with respect to the vertical, or crush, direction. A photograph of a typical conusoid component is shown in Figure 3(b). Dimensions of the component are 12-in. long, 7.5-in. high, with an overall width of 1.5-in. Additional information on the development and fabrication of the conusoid energy absorber may be found in Reference 6.

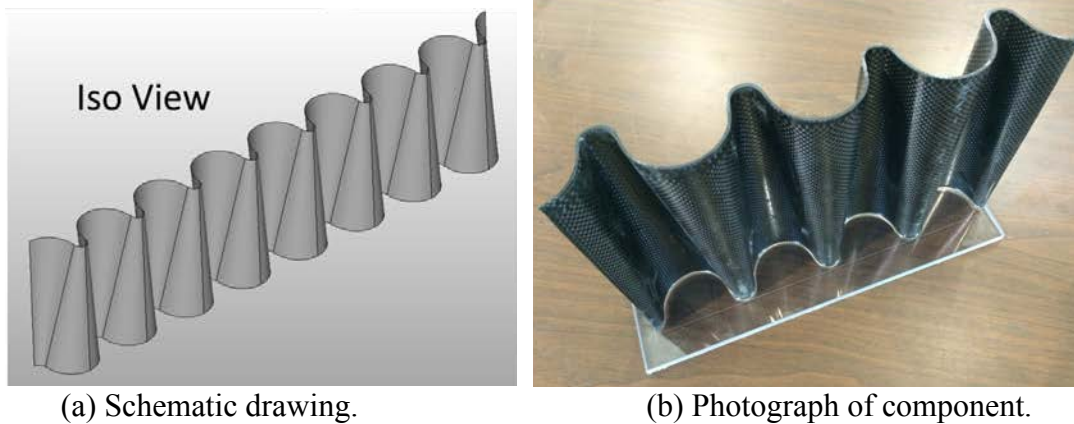(a) Schematic drawing.   (b) Photograph of component.

Figure 3. Isometric view and photograph of a conusoid component.

3.3 Sinusoid Foam Sandwich Energy Absorber

The second energy absorber, designated the "sinusoid," consisted of hybrid carbon-Kevlar® plain weave fabric face sheets, two layers for each face sheet oriented at ±45° with respect to the vertical, or crush, direction and a closed-cell ELFOAM® P200 polyisocyanurate (2.0-lb/ft^3) foam core. Sine wave energy absorbers have been studied extensively because they offer desirable features under compressive loading [19-22]. Energy absorption values from sine wave concepts can be similar to

4

values obtained from crush tubes. In addition, sine wave concepts tend to deform in a stable manner through plastic hinge formation and crushing, rather than global buckling. Often, the actual shape of the energy absorber is not truly a sine wave, but a series of alternating half circles. In fact, the sinusoid concept described in this paper is actually a series of half circles with a diameter of 1.75-in.; however, the designation of "sinusoid" will continue to be used.

The total thickness of a sinusoid component was 1.5-in. with a length of 12-in. and a height of 7.5-in. Design parameters were assessed through component testing including different materials for the face sheets and different laminate stacking sequences. Variations in sinusoid geometry were not evaluated since an existing mold was used in construction. A photograph of a sinusoid foam sandwich specimen is shown in Figure 4. Note that, in preparation for the component drop test, 0.5-in.-thick polycarbonate plates were attached to both the top and bottom surfaces of the specimen.
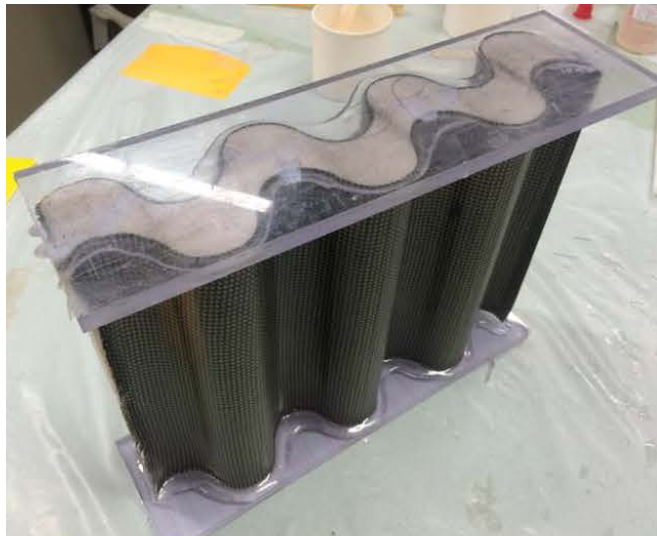

Figure 4. Pre-test photograph of a sinusoid foam sandwich component.

4.0 COMPONENT TESTING AND SIMULATION

4.1 Conusoid Energy Absorber

Different conusoid energy absorber designs were dynamically crushed in a 14-ft. drop tower with an instrumented 110-lb. falling mass. The impact condition for all of the dynamically crushed specimens was approximately 264-in/s (22-ft/s). The drop mass was instrumented with a 500-g damped accelerometer and data were acquired using a National Instruments Data Acquisition System (DAS) sampling at 25-kHz. All post-processed acceleration data were filtered using a low-pass 4-pole Butterworth filter with a 500-Hz cutoff frequency. A high-speed camera filming at 1-kHz captured the deformation time history, which is depicted in Figure 5. The identified failure mechanism is folding of the conusoid walls, which is a desirable failure mode that produces a stable and constant crush response within the design level of 25-40 g.

A depiction of the finite element model representing the conusoid energy absorber is shown in Figure 6. The model contained 185,940 nodes; 44,294 Belytschko-Tsay shell elements; 116,100 solid elements representing the rigid drop mass, 1 initial velocity card assigned to nodes forming the rigid mass, and 1 body load card defining gravity. The nominal shell element edge length is 0.032-

in. The shell elements representing the hybrid carbon-Kevlar® fabric layers were assigned Mat 58, which is a continuum damage mechanics material model used in LS-DYNA® for representing composite laminates and fabrics [23].
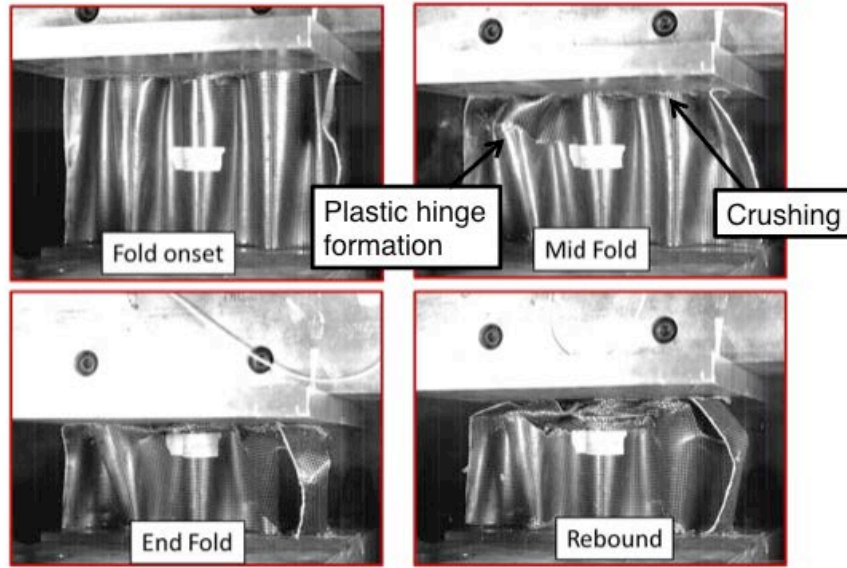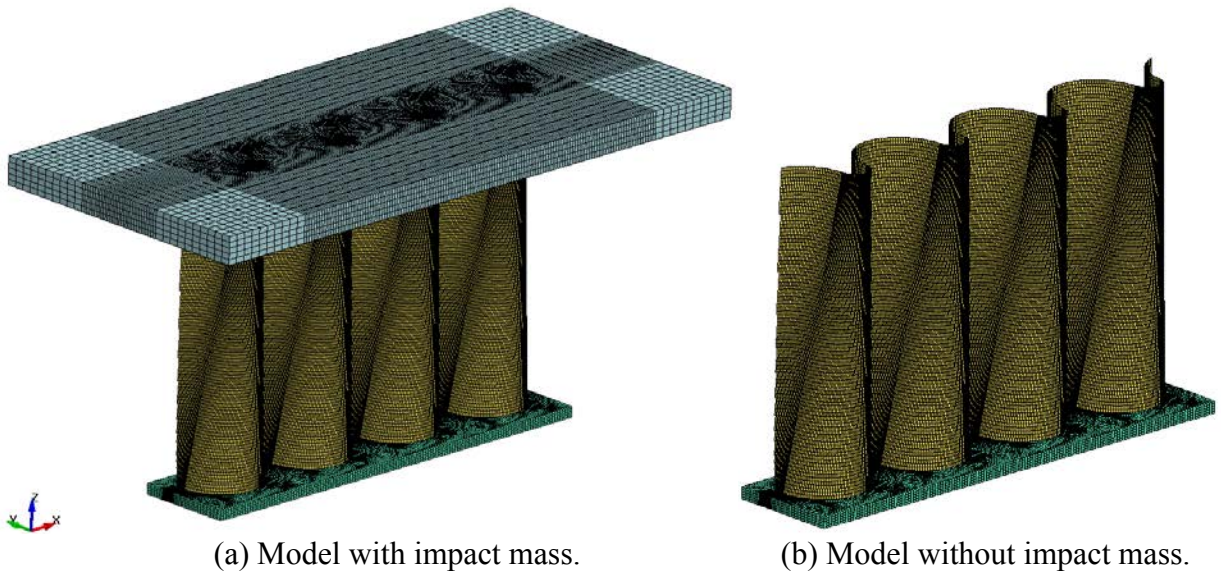

Figure 5. High-speed video clips of conusoid deformation.

(a) Model with impact mass. (b) Model without impact mass.

Figure 6. Depictions of the conusoid component model.

Baseline Mat 58 properties are listed in Table 1. Properties for Mat 58 were obtained through detailed test-analysis comparisons with experimental data obtained from standard material characterization tests, such as tensile testing of fabric coupons oriented at 0°, 90°, and ±45° to obtain longitudinal stiffness and strength, transverse stiffness and strength, and shear stiffness and strength, respectively. Once verified through comparison with coupon test data, these properties were unchanged for all subsequent simulations of the energy absorbers. It should be noted that Mat 58 includes certain parameters, such as the SLIM parameters and ERODS, that cannot be determined entirely based on experimental data. For these parameters, estimates were input based

on past experience of the analysts. For the conusoid, individual ply layers were input using the *PART_COMPOSITE feature in LS-DYNA® which allows input of ply orientations, ply thicknesses, and ply material designations for each layer within a composite laminate. Single Point Constraints (SPCs) were used to constrain the nodes forming the bottom plate. The conusoid model was executed using LS-DYNA® SMP version 971 on a Linux-based workstation with 8 processors and required 11 hours and 49 minutes of clock time to execute the simulation for 0.035-seconds. Model output included time-history responses of the drop mass, and image sequences of structural deformation.

Table 1. Mat 58 material properties used to represent hybrid carbon-Kevlar® fabric.

Material Property Description	Symbol	Values
Density, lb-s^2/in^4	RO	0.903E-4
Young's modulus longitudinal direction, psi	EA	6.3E+6
Young's modulus transverse direction, psi	EB	2.76E+6
Poisson's ratio, v_{21}	PRBA	0.03
Stress limit of nonlinear portion of shear curve, psi	TAU1	4,500.
Strain limit of nonlinear portion of shear curve, in/in	GAMMA1	0.06
Shear modulus AB, BC, and CA, psi	GAB	3.0E+5
Min stress factor for limit after max stress (fiber tension)	SLIMT1	0.8
Min stress factor for limit after max stress (fiber comp)	SLIMC1	1.0
Min stress factor for limit after max stress (matrix tension)	SLIMT2	0.8
Min stress factor for limit after max stress (matrix comp)	SLIMC2	1.0
Min stress factor for limit after max stress (shear)	SLIMS	1.0
Material axes option (model dependent)	AOPT	0.0
Maximum effective strain for element layer failure	ERODS	0.5
Failure surface type	FS	-1.0
Strain at longitudinal compressive strength, in/in	E11C	0.007
Strain at longitudinal tensile strength, in/in	E11T	0.0143
Strain at transverse compressive strength, in/in	E22C	0.012
Strain at transverse tensile strength, in/in	E22T	0.025
Strain at shear strength, in/in	GMS	0.45
Longitudinal compressive strength, psi	XC	40,000.
Longitudinal tensile strength, psi	XT	89,000.
Transverse compressive strength, psi	YC	25,000.
Transverse tensile strength, psi	YT	54,000.
Shear strength, psi	SC	7,100.

Comparisons of predicted and experimental acceleration and displacement time histories of the drop mass are shown in Figures 7(a) and (b), respectively. The conusoid model over predicts the magnitude of the initial peak acceleration, 96-g compared with 61-g for the test. However, other than that anomaly, the level of agreement is good. The average acceleration calculated for the test is 28.0-g for pulse duration of 0.0- to 0.025-s, whereas the model average acceleration is 28.4-g for the same duration. The results of the conusoid component test indicate that the configuration of the energy absorber meets all of the design goals, including achieving a sustained average acceleration level of between 25-40-g. The comparison of vertical displacement time histories also exhibits good agreement, as shown in Figure 7(b). The maximum displacement of the test article is 2.9-in., providing a crush stroke of 38.7%. The maximum displacement of the model is 2.53-in., providing a

crush stroke of 33.7%. Note that the entire range of crush stroke was not evaluated during component testing.

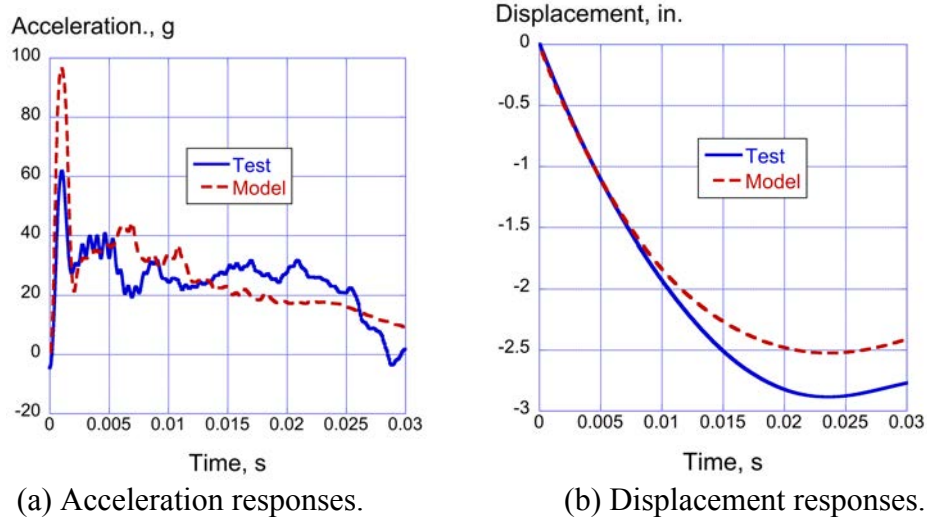(a) Acceleration responses.   (b) Displacement responses.

Figure 7. Acceleration and displacement comparisons for the conusoid component vertical drop test.

A sequence of model deformation is shown in Figure 8. Stable crushing occurs through plastic hinge formation and folding, along with some local buckling of the conusoid walls. The predicted response matches the model deformation captured by the high-speed camera, as shown in Figure 5. Note that the ERODS parameter is set to 0.5 (see Table 1), indicating that elements are deleted from the simulation once they reach an effective strain of 50%. If the erosion parameter is set too low, holes produced in the model by element deletion could lead to premature failure and unstable model behavior.
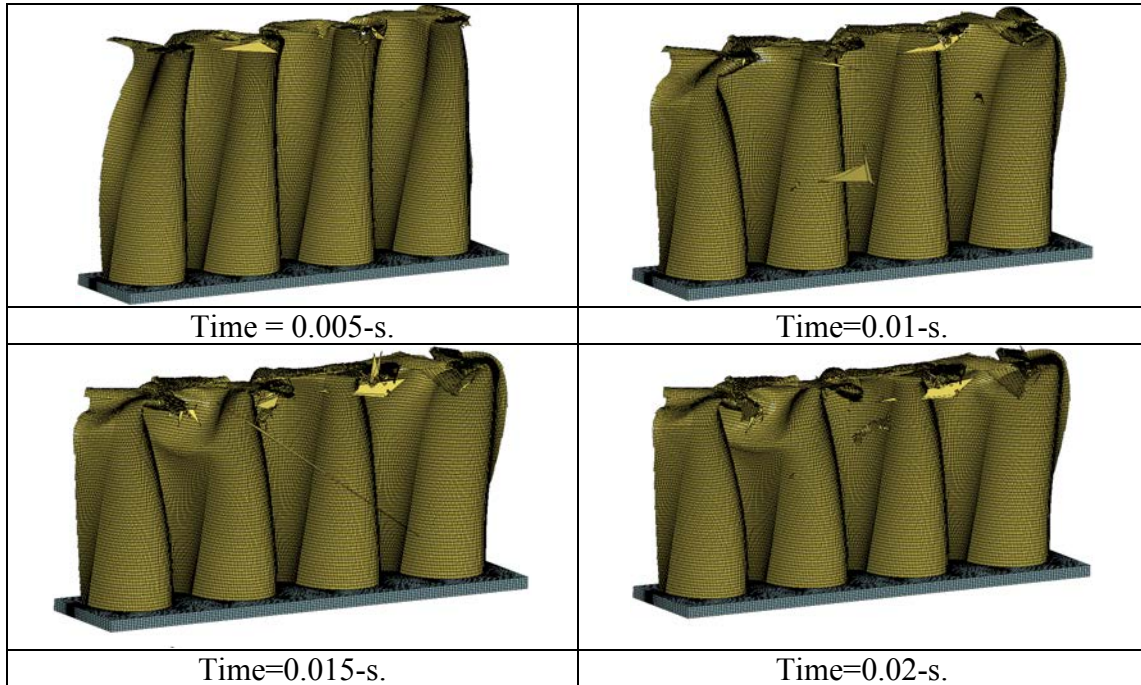

| Time = 0.005-s. | Time=0.01-s. |
| Time=0.015-s. | Time=0.02-s. |

Figure 8. Deformation sequence of the conusoid. Note that deleted elements are highly distorted.

4.2 Sinusoid Energy Absorber

The sinusoid foam sandwich energy absorber was initially evaluated through quasi-static and dynamic crush testing of components. A post-test photograph of a typical sinusoid component is shown in Figure 9 for a dynamic crush test in which a 113.5-lb mass impacted the sinusoid at 265-in/s (22.08-ft/s). The sinusoid component is approximately 12-in. long, 7.5-in. high, and 1.5-in. wide. A flat 0.5-in.-thick polycarbonate plate was glued to both the top and bottom surfaces of the specimen. As shown in Figure 9, the specimen exhibits stable, plastic-like deformation with uniform folding of the face sheets and crushing of the foam core. Crushing initiates along the top edge of the specimen. Note that the sides of the specimen were not covered with face sheets, which allowed splaying of the foam core.

The LS-DYNA® finite element model representing the sinusoid component drop test is shown in Figure 10. The model contained: 53,540 nodes; 7,380 Belytschko-Tsay shell elements; 37,515 solid elements; a rigid drop mass; 1 initial velocity card assigned to nodes forming the rigid drop mass; SPCs to fully constrain the bottom nodes of the sinusoid; 1 automatic single surface contact; and 3 material definitions. As with the conusoid, the shell elements were assigned Mat 58, using the properties listed in Table 1. The nominal element edge length in the sinusoid model was 0.2-inches.
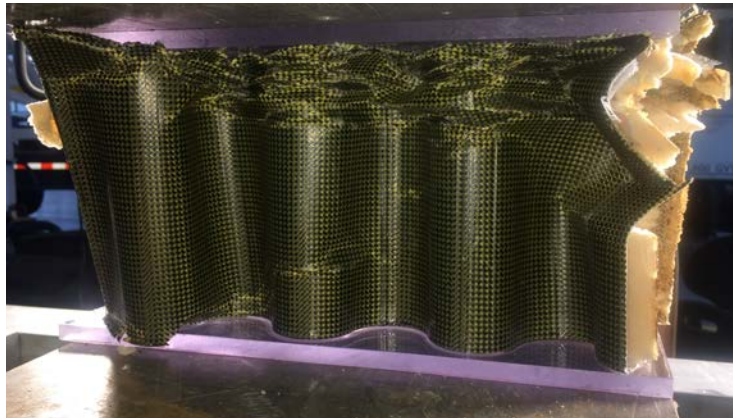

Figure 9. Post-test photograph of a sinusoid foam sandwich energy absorber.

The solid elements representing the foam core were assigned Mat 63, which is a crushable foam material model in LS-DYNA® that allows user input of the stress-strain response of the material in tabular format. The stress-strain response of the P200 foam was determined through quasi-static testing of 4-in. x 4-in. x 3-in. rectangular blocks. A plot of the experimental curve obtained at a crush rate of 1.0-in/minute is shown in Figure 11, along with the stress-strain response used as input to Mat 63. Note that the input curve matches the test data to a strain of 0.67-in/in. At this point, the test data ends, yet the Mat 63 input response continues and increases dramatically up to 100,000-psi at 1-in/in (note that this data point is not shown in the plot). The large "tail" added to the end of the stress-strain response represents compaction of the foam and is needed to stabilize the response of the solid elements for high values of volumetric strain.
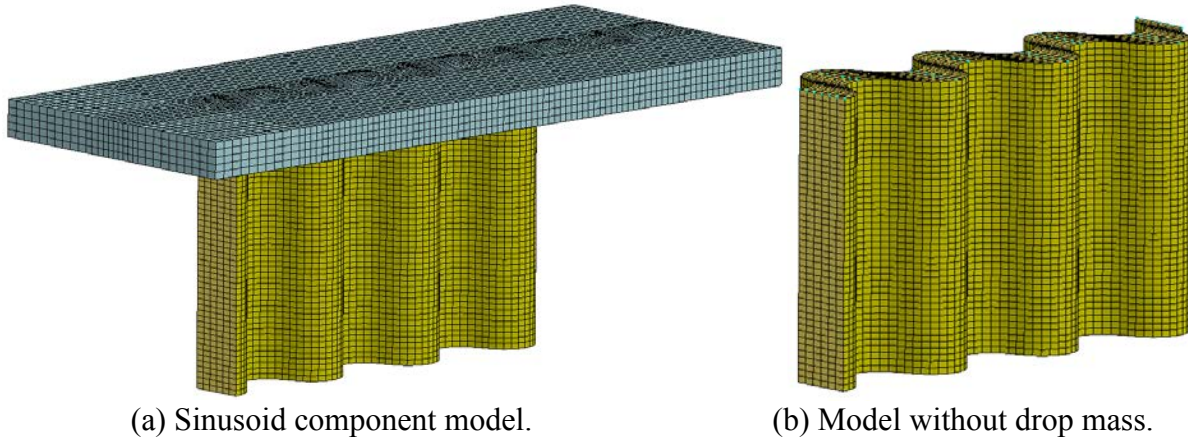
(a) Sinusoid component model.   (b) Model without drop mass.

Figure 10. Depictions of the finite element model of the sinusoid component.

The sinusoid model was executed using LS-DYNA® SMP version 971 on a Linux-based workstation with 8 processors and required 10 hours and 34 minutes of clock time to execute the simulation for 0.04-seconds. Model output included time-history responses of the drop mass, and image sequences of structural deformation.
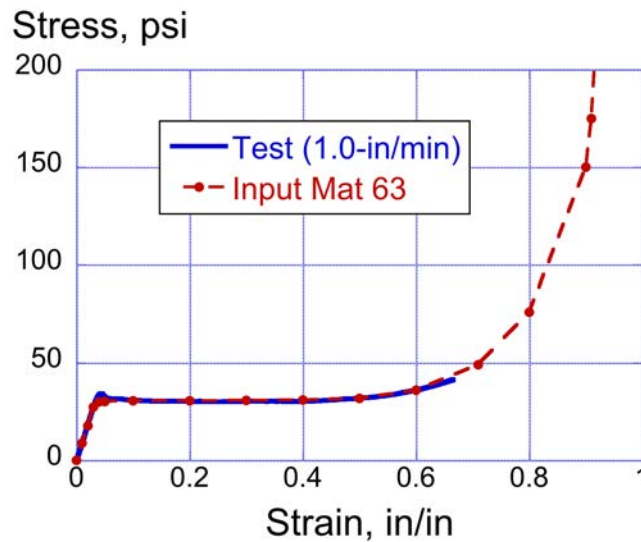

Figure 11. Plot of P200 foam stress-strain response.

Test-analysis comparisons of time-history responses are plotted in Figure 12 for the sinusoid component crush test. These results demonstrate excellent test-analysis agreement. As can be seen in Figure 12(a), the acceleration response of the drop mass achieves an initial peak of 55-g, then drops to approximately 22-g, where it remains constant until the end of the pulse. The model mimics this response, even predicting the unloading response near the end of the pulse. The average acceleration calculated for the test is 21.8-g for pulse duration of 0.0- to 0.03-s, whereas the average acceleration of the predicted response is 22.9-g for the same duration. The experimental and analytical displacement responses, shown in Figure 12(b), exhibit maximum values of 4- and 3.8-in., respectively, which represents approximately 50% stroke. The average acceleration results for the sinusoid fall slightly below the required design goal of 25- to 40-g. The lower average crush acceleration for the sinusoid translates into a larger crush stroke than was seen for the conusoid.

10

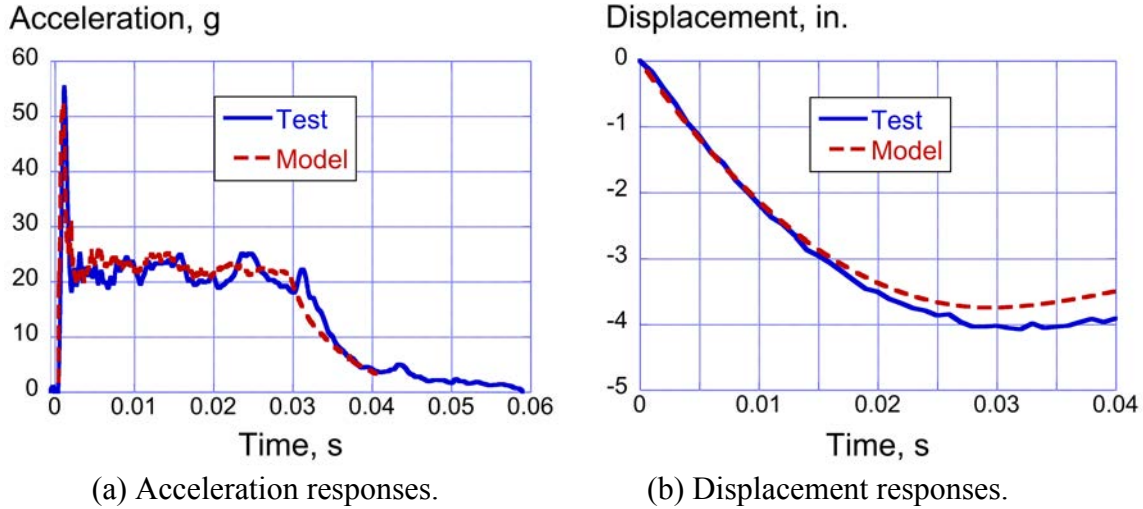(a) Acceleration responses.   (b) Displacement responses.

Figure 12. Test-analysis time history comparisons for the sinusoid component.

The predicted sinusoid model deformation is shown in Figure 13 for six discrete time steps. The model exhibits stable crushing through folding and plastic-like deformation of the face sheets and crushing of the foam core. The deformation pattern matches the test response shown in Figure 9.
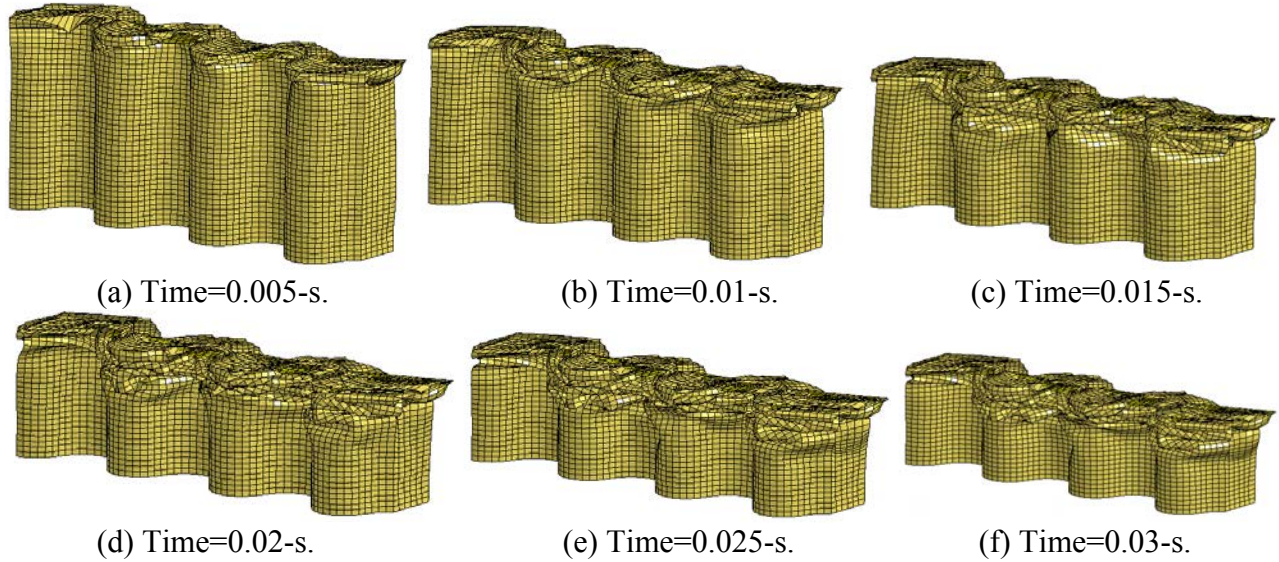

(a) Time=0.005-s.   (b) Time=0.01-s.   (c) Time=0.015-s.

(d) Time=0.02-s.   (e) Time=0.025-s.   (f) Time=0.03-s.

Figure 13. Predicted sinusoid model deformation.

5.0 RETROFITTED BARREL SECTION DROP TESTING AND SIMULATION

5.1 Experimental Program

Following the TRACT 1 crash test, a portion of the forward cabin (Fuselage Station FS164 through FS250) was separated from the remainder of the post-test specimen. The resulting barrel section was essentially undamaged during the TRACT 1 test and was retrofitted with two of the energy absorbing concepts planned for TRACT 2, including the conusoid and the sinusoid foam sandwich designs. The original floor in the barrel section was removed and was replaced with a sheet of 0.5-in.-thick polycarbonate. The reason for this change was to enable viewing of the crushing response of the energy absorbers using high-speed cameras. The total weight of the fully loaded barrel

11

section was 1,810-lb. It was impacted onto concrete at 297.6-in/s (24.8-ft/s). The objectives of the barrel section test were to evaluate: (1) the performance of the two energy absorbers during a full-scale drop test prior to the TRACT 2 test, (2) the fabrication methods for the energy absorbers, (3) the structural integrity of the retrofit, (4) the strength of the polycarbonate floor, and (5) imaging techniques used during the test.

Pre-test photographs of the barrel section test article are shown in Figures 14(a) and (b), highlighting front and rear views, respectively. Close-up photographs showing the conusoid and sinusoid foam sandwich energy absorbers that were retrofitted into the barrel section are shown in Figures 15(a) and (b), respectively. The conusoid subfloor was located at FS220. The floor of the fuselage section was loaded with a 681-lb concentrated mass, which was centered about FS220 and located just above the conusoid energy absorber. The sinusoid energy absorber was located at FS190, in front of the conusoid. Both energy absorbers were painted white and vertical tick marks were added to aid in deformation tracking.

The floor of the fuselage section was loaded with a 320-lb concentrated mass on the right-hand side and a double seat with two 50th percentile male Anthropomorphic Test Devices (ATDs) on the left-hand side, both centered about FS190 and located just above the sinusoid energy absorber. The seat was attached to the floor using standard seat tracks and the seated dummies were restrained using lap belts only. The combined weight of the seat and dummies was 405-lb. This loading condition was intended to replicate the anticipated TRACT 2 configuration.

| (a) Front view. | (b) Rear view. |

Figure 14. Front and rear view photographs of the CH-46E barrel section.

The barrel section test was conducted by raising the test article to a height of 115.2-in. (9.6-ft) and releasing it to impact a concrete surface at 297.6-in/s (24.8-ft/s). Data were collected at 25-kHz primarily from accelerometers located throughout the cabin and on the 320- and 681-lb masses.

(a) Photograph of the conusoid energy absorber.

(b) Photograph of the sinusoid foam sandwich energy absorber.

Figure 15. Pre-test photographs of the conusoid and sinusoid energy absorbers, as retrofitted into the barrel section.

A post-test photograph highlighting the crushing response of the conusoid energy absorber is shown in Figure 16. The original height of the conusoid was 8.31-in., as measured at the center of the subfloor, and the post-test height was 3.44-in., providing a crush stroke of 58%. As seen in Figure 16, the conusoid energy absorber displayed fracturing and delamination of the hybrid carbon-Kevlar® plies. Most of the damage was located in the center of the specimen, under the 681-lb mass.

Figure 16. Post-test photograph of the conusoid energy absorber.

Post-test photographs of the barrel section and the sinusoid energy absorber are highlighted in Figure 17. The original height of the sinusoid energy absorber was 8.75-in., as measured at the center of the subfloor, and the post-test height was 4.44-in., providing a crush stroke of 49.3%. As seen in Figure 17(b), the sinusoid foam sandwich energy absorber displayed crushing of the foam core, and fracturing of the face sheets starting from the bottom, curved edge. The sinusoid energy absorber in the barrel section did not exhibit the uniform folding pattern seen in the face sheets of the component specimen.

One issue with the barrel section drop test was noted following the impact event. Two 0.5-in.-diameter steel bolts were used to attach the 320-lb mass to the polycarbonate floor of the section. These bolts were approximately 12-in. in length, and one bolt was located 12-in. in front of the other. After drilling through the lead mass and floor, the bolts extended approximately 3.5- to 4-in. into the subfloor crush zone. The extra bolt lengths were not trimmed prior to the test and the bolts

impacted the bottom skin of the fuselage section during the test. The forward bolt can be seen highlighted on the left side of Figures 15(b) and 17(b). Following the test, the bolts were removed and they are depicted in the photograph of Figure 18. The forward bolt impacted the fuselage skin and deformed plastically. Much less permanent deformation is seen in the second bolt. The presence of these bolts affected the acceleration response of the 320-lb mass during the latter portion of the time history response, which will be discussed later in the paper.

(a) Post-test photograph of the barrel section.

(b) Post-test photograph highlighting the post-test crush response of the sinusoid.

Figure 17. Post-test photographs of the barrel section drop test.
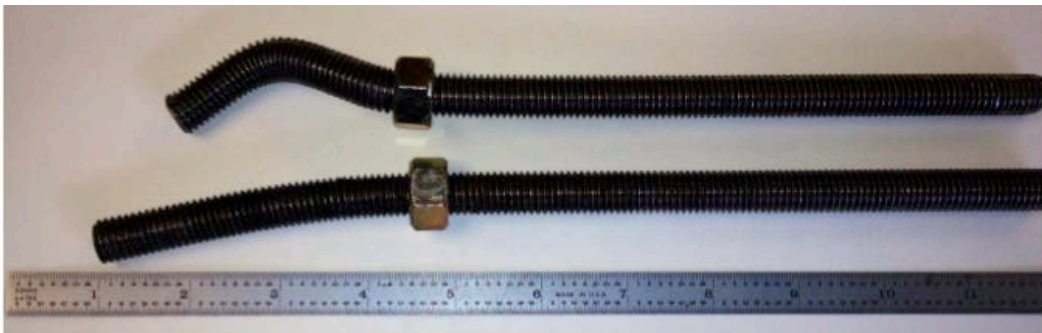
Figure 18. Post-test photograph of exposed steel bolts.

5.2 Barrel Section Finite Element Model

The finite element model of the barrel section is shown in Figure 19. This model contains: 105,986 nodes; 22 parts; 10 material definitions; 57,041 Belytschko-Tsay shell elements; 63,591 solid elements; 1,677 beam elements; 1 initial velocity; 1 contact definition; 20 discrete masses representing the double seat and ATD occupants; 2 lumped masses representing the 320- and 681-lb

14

blocks used in the test article; and 1 planar rigid wall representing the impact surface, which is not shown in Figure 19. The seat and occupants were represented using 20 discrete masses assigned to nodes at the approximate seat track attachment locations. All nodes in the barrel section model were assigned an initial velocity of 297.6-in/s (24.8-ft/s), matching the measured test velocity. The hybrid carbon-Kevlar® fabric material, used in the construction of the conusoid and the face sheets of the sinusoid foam sandwich energy absorbers, was represented using Mat 58 in LS-DYNA® (see property values listed in Table 1). The aluminum outer skin and frames were assigned properties of Mat 24, an elastic-plastic material model. The steel bolts were simulated using beam elements that were assigned material properties of hardened steel.

A depiction of the model of the conusoid energy absorber is shown in Figure 20(a). The conusoid was constructed of four layers of hybrid carbon-Kevlar® plain weave fabric with a stacking sequence of [+45°/-45°/-45°/+45°]. The individual ply orientations and thicknesses were input using the *PART_COMPOSITE command in LS-DYNA®. A nominal element edge length of 0.3-in. was used in the conusoid mesh. The finite element model of the sinusoid subfloor is shown in Figure 20(b). As before, the face sheets were represented as two layers of hybrid carbon-Kevlar® plain weave fabric with a stacking sequence of [±45°] that were assigned Mat 58 material properties (see Table 1). The solid elements representing the foam core were assigned Mat 63. A nominal element edge length of 0.25-in. was used in the sinusoid mesh. Note that in the test article, the energy absorbers were attached to the outer skin and floor using rivets. In the model, the rivets were not physically modeled; however, coincident nodes were used to tie the parts together.

An automatic single surface contact was assigned to the model with static and dynamic coefficients of friction of 0.3. This general contact definition is used to prevent any node from penetrating any element within the model. The model was executed using LS-DYNA® SMP version 971 on a Linux-based workstation with 8 processors and required 31.75 hours of clock time to execute the simulation for 0.065-seconds. Model output included time-history responses of the 320- and 681-lb lumped masses, and image sequences of structural deformation.
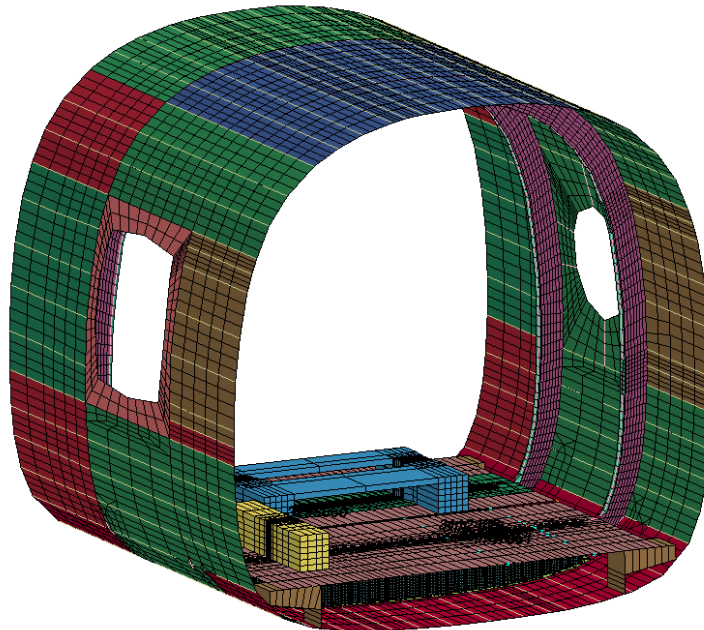

Figure 19. Finite element model of the CH-46E barrel section.

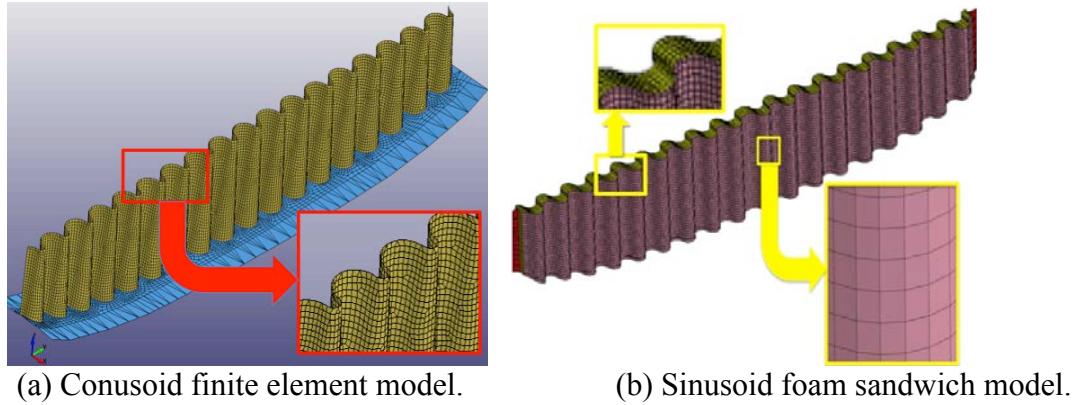(a) Conusoid finite element model.   (b) Sinusoid foam sandwich model.

Figure 20. Depictions of the finite element models of the two energy absorbing subfloors.

5.3 Barrel Section Test-Analysis Comparisons

Test-analysis time history responses of the 681-lb mass, located above the conusoid energy absorber, are plotted in Figure 21. The predicted acceleration response shows a spike that occurs at 0.032-s. This spike is attributed to bottoming out of the subfloor section, meaning that the floor impacts the outer skin of the fuselage section. The "bottoming out" response was confirmed when viewing the high-speed video. The test acceleration response also indicates that the subfloor bottomed out, as evident by the gradual increase in acceleration leading to a 34.5-g peak near the end of the pulse. Average accelerations of 15.0- and 20.3-g were calculated for the test and predicted responses, respectively, for a pulse duration of 0.0- to 0.06-s. The selection of the pulse duration for calculating average acceleration was made based on the time at which both acceleration traces were approaching zero magnitude. The velocity responses indicate that the model is too stiff and predicted velocity is removed much more quickly than for the test. In addition, the model predicts a much higher rebound velocity than the test, which indicates that the model contains too much elastic energy and that the unloading response is not adequately captured. The predicted maximum crush displacement is 7.8-in. and the experimental maximum crush displacement is 8.67-in., a difference of approximately 0.9-in. Finally, it should be noted that the average test acceleration response falls below the design goal of 25- to 40-g.

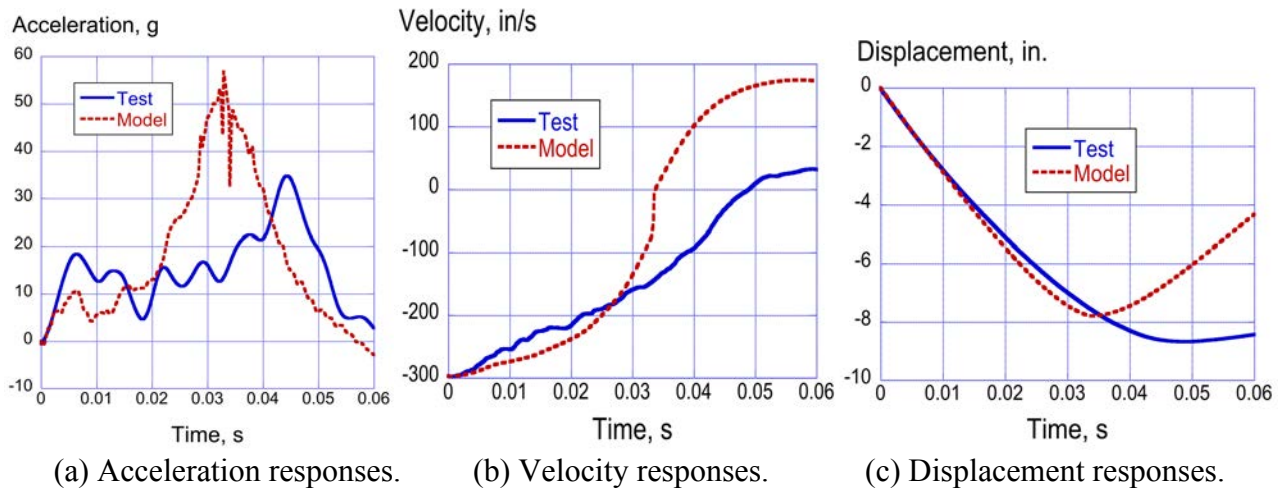(a) Acceleration responses.   (b) Velocity responses.   (c) Displacement responses.

Figure 21. Comparisons of test-analysis responses of the 681-lb mass over the conusoid subfloor.

A time sequence of predicted deformations is shown in Figure 22 for the conusoid subfloor beam. Initially, the crush pattern is non-uniform due to the fact that the 681-lb mass is actually attached to the floor using two I-beams separated by 26-in. with flange widths of 6-in. The sides of the conusoid subfloor that attach to the fuselage frames are relatively undamaged. Finally, a post-test photograph of the conusoid subfloor, which was removed from the test article, is shown in Figure 23. The deformation and failure pattern is more uniform, especially in the central portion of the subfloor than predicted. It is also interesting to note the permanent deformation pattern of the polycarbonate floor above the conusoid.

(a) Time=0.01-s.

(b) Time=0.02-s.

(c) Time=0.03-s.

(d) Time=0.04-s.
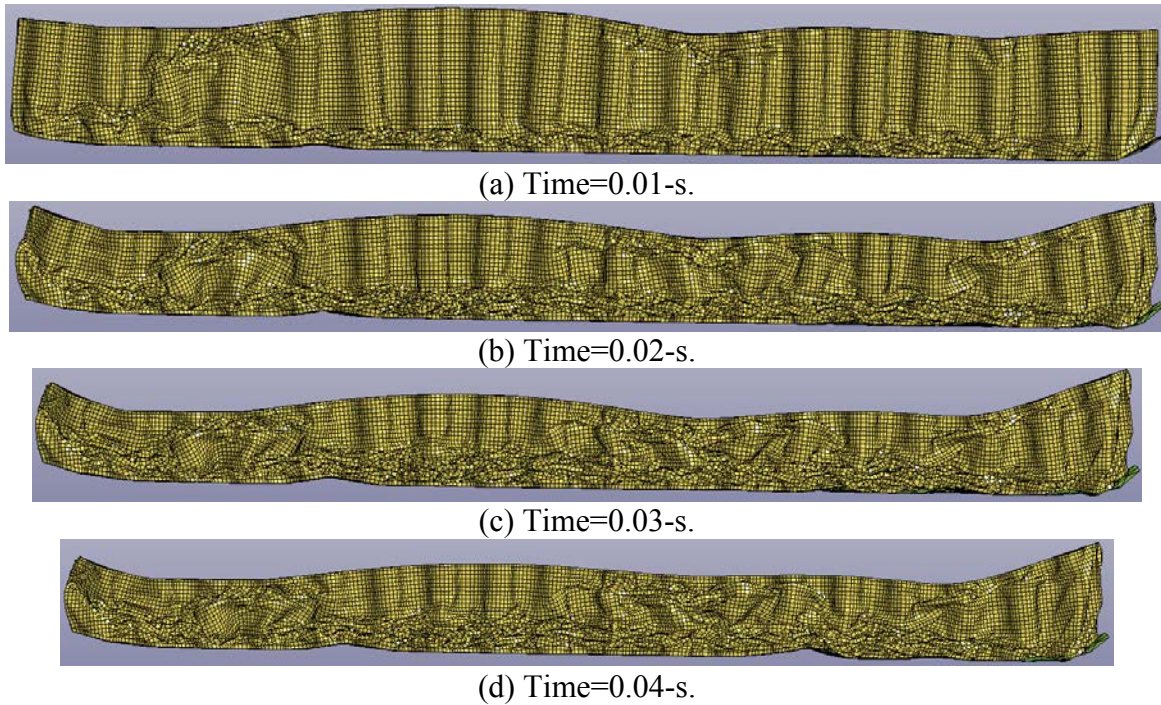
Figure 22. Predicted deformation pattern of the conusoid subfloor.

Figure 23. Photograph of the conusoid energy absorber, removed from the test article. Note that the conusoid is lying on its side with a portion of the polycarbonate floor still attached.

Test-analysis time-history responses of the 320-lb mass, located above the sinusoid energy absorber, are plotted in Figure 24. While the predicted responses demonstrate reasonable comparison with test, the model fails to predict the large increase in acceleration that occurs just prior to 0.03-s. This 64-g peak is attributed to impact of the steel bolts with the outer skin. Even though the model includes the bolts, the predicted acceleration response does not match the test. Average accelerations of 14.2- and 17.0-g were calculated for the test and predicted responses, respectively, for a pulse duration of 0.0- to 0.0575-s. It should be noted that average test and predicted accelerations are well below the design goal of 25- to 40-g. The test-analysis velocity responses are shown in Figure 24(b), both of which cross zero at the same time (0.0326-s), even

17

though the test and predicted curves deviate shortly after 0.01-s. The model predicts a much higher rebound velocity than the test, which indicates that the model returns too much elastic energy and that the unloading response is not adequately represented. The predicted maximum crush displacement is 5.24-in. and the experimental maximum crush displacement is 6.3-in., a difference of approximately 1-in.
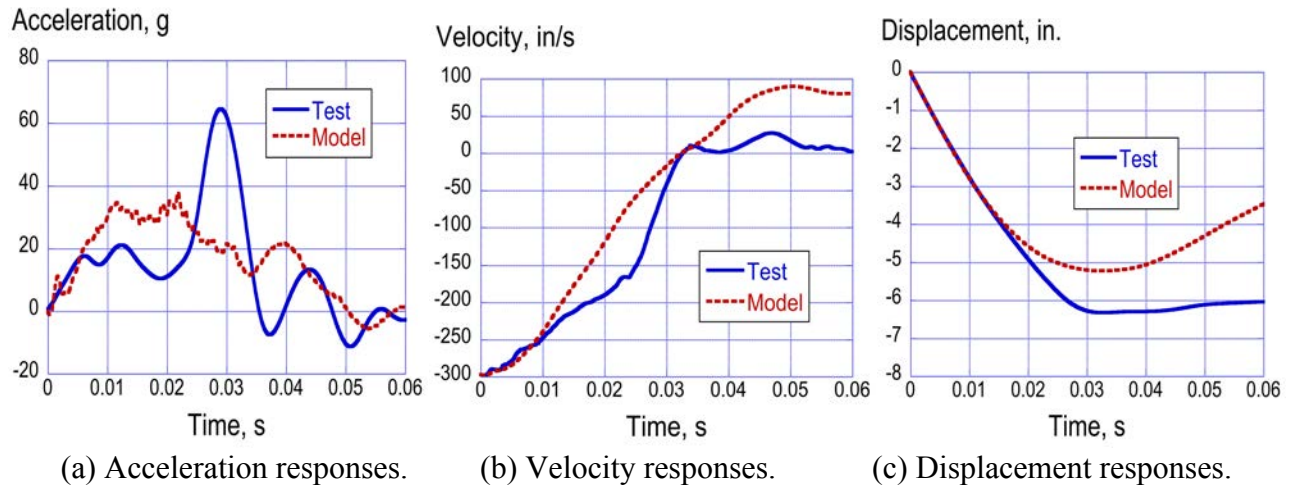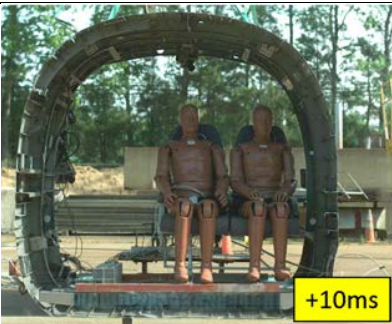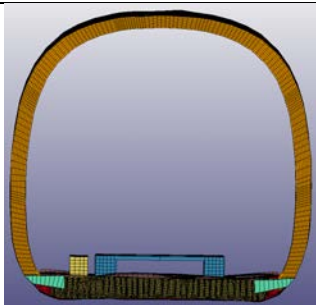

(a) Acceleration responses.   (b) Velocity responses.   (c) Displacement responses.

Figure 24. Comparisons of experimental and predicted responses of the 320-lb mass.

Three images from the high-speed video are compared with predicted model deformation in Figure 25 at times of 0.01-, 0.03-, and 0.043-s. By 0.043-s, fairly severe deformations are evident in the upper portion of the fuselage section. This deformation is asymmetric, located on one side only, and is not captured by the model. While the model exhibits some oscillatory motion in the outer skin, it does not show the large deformation evident in the test. It should be noted that the deformation in the test article is elastic, since the upper fuselage section returns to its normal shape by the end of the pulse, as indicated in the post-test photograph shown in Figure 17(a).

A time sequence of predicted sinusoid foam sandwich deformations is shown in Figure 26. Initially, the crush pattern is non-uniform due to the fact that the subfloor is loaded by two discrete masses, the 320-lb mass on one side and the seat and occupants on the other. Note that the sides of the sinusoid subfloor that attach to the fuselage frames are relatively undamaged. Finally, a post-test photograph of the sinusoid subfloor, which was removed from the test article, is shown in Figure 27. The deformation and failure pattern of the sinusoid is more uniform than the predicted response; however, the locations and types of damage are similar.
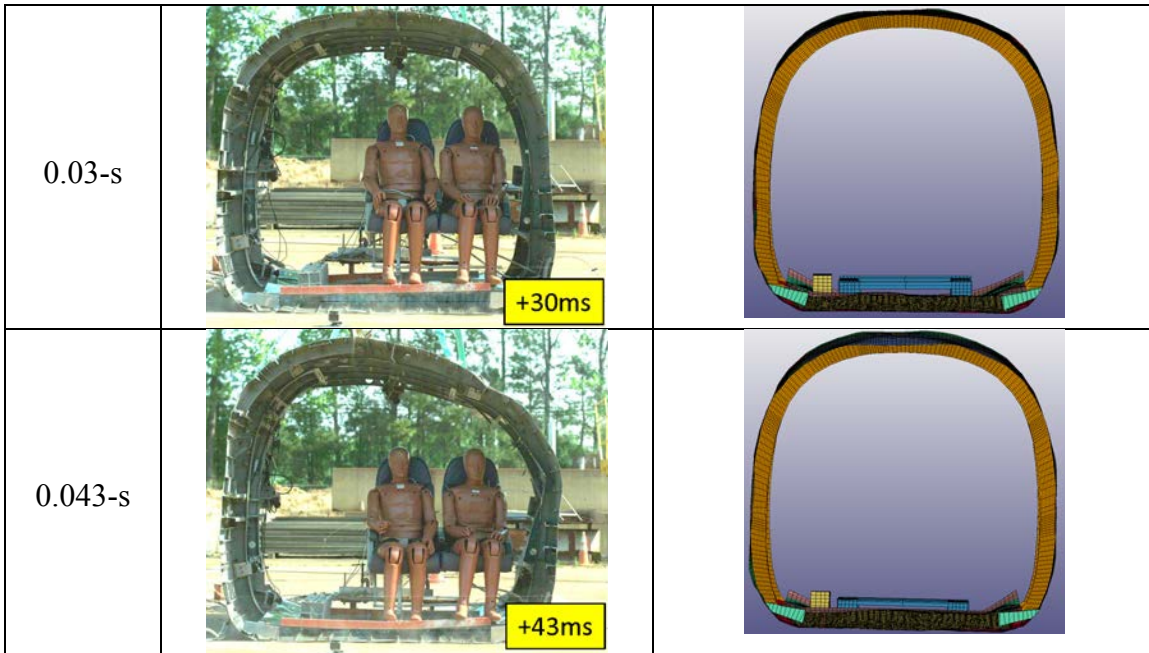
Time, s	Test	Model
0.01-s		

0.03-s		
0.043-s		

Figure 25. Comparison of experimental and predicted deformation patterns.

(a) Time=0.0-s.

(b) Time=0.01-s

(c) Time=0.02-s.
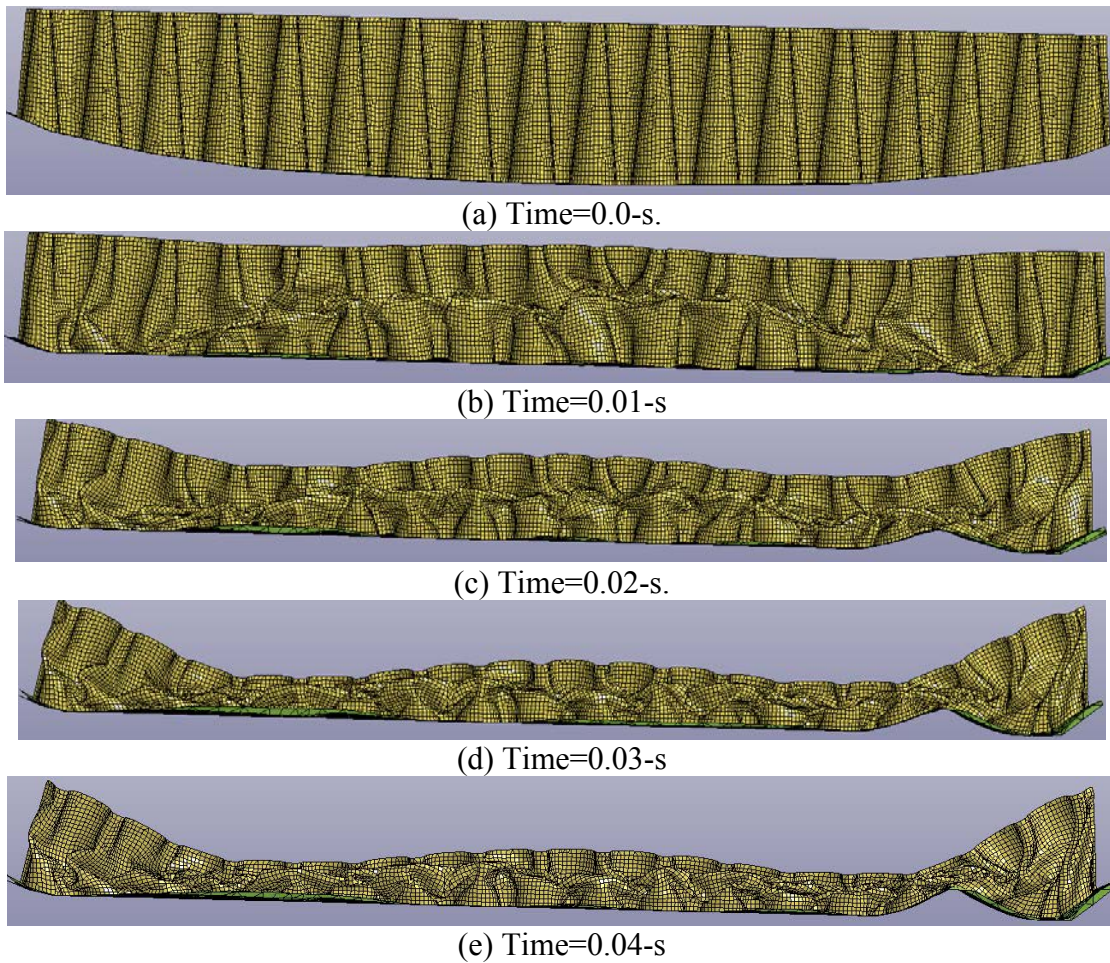

(d) Time=0.03-s

(e) Time=0.04-s

Figure 26. Predicted deformation pattern of the sinusoid foam sandwich subfloor.

Figure 27. Photograph of the sinusoid foam sandwich energy absorber, removed from the test article. Note that the subfloor section is lying on its side with a portion of the polycarbonate floor still attached.

6.0 FULL-SCALE CRASH TESTING AND SIMULATION OF TRACT 2

6.1 TRACT 2 Full-Scale Crash Test

A second CH-46E helicopter airframe was prepared for crash testing and loaded in a similar manner as the TRACT 1 test article [2]. In addition, the TRACT 2 aircraft was retrofitted with three different composite energy absorbing subfloor concepts [3]. The shear panel at FS220 was replaced with a corrugated web energy absorber developed by the German DLR and the Australian ACS-CRC and fabricated of graphite fabric material [4, 5]. The shear panel at FS254 was replaced with the sinusoid foam sandwich energy absorber and the shear panel at FS286 was replaced with the conusoid energy absorber [6]. A photograph showing the retrofit of the sinusoid and conusoid energy absorbers into the TRACT 2 subfloor is shown in Figure 28. Unlike the barrel section, the original floor in the CH-46E was not replaced with polycarbonate material. However, for viewing of the subfloor response during the crash test, rectangular-shaped windows were cut into the floor panels at discrete locations between the seat rails and polycarbonate was used to fill these openings. Photographs of the conusoid and sinusoid energy absorbers are shown in Figures 29(a) and (b), respectively, as viewed through the polycarbonate windows. The energy absorbers were 63-in. wide, 9.2-in. tall, and 1.5-in. deep. The conusoid and sinusoid subfloor beams weighed 4.02- and 4.52-lb., respectively. In comparison, the aluminum shear panel that was replaced weighed 5.75-lb.
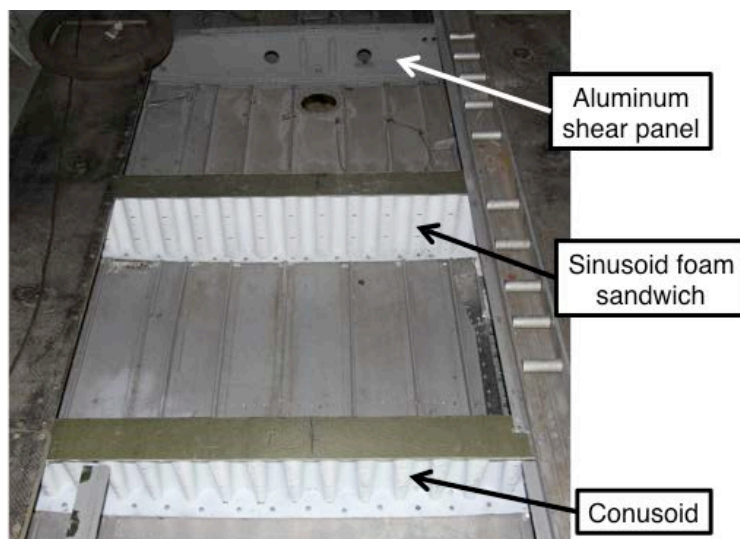

Figure 28. Photograph showing the retrofitted sinusoid and conusoid energy absorbers.

20

On October 1, 2014, the TRACT 2 full-scale crash test was conducted at the LandIR Facility. Pre- and post-test photographs are shown in Figure 30. Nine organizations, including NASA, NAVAIR, DLR/ACS-CRC, FAA, US Army Aeromedical Research Laboratory (USAARL), US Army CARGO, Cobham Life Support/BAE Systems, and Safe Inc., took part in the TRACT 2 activity, contributing 18 experiments related to occupant seating and restraints, composite crashworthiness, and emergency locator transponder survivability, as described in References 3 and 24-27. The TRACT 2 test article was instrumented with over 360 data channels, including 13 ATDs, 12 on-board high-speed cameras, 10 on-board Go-Pro cameras, and 12 external high-speed cameras. Data were recovered from over 95% of the channels, with only one on-board high-speed camera and two Go-Pro cameras failing to operate. Measured impact conditions were 403.8-in/s (33.65-ft/s) forward velocity and 304.32-in/s (25.36-ft/s) vertical velocity. The airframe attitude at impact was 2.6° pitch (nose up) and 3.5° roll (left side down). The total weight of the test article was 10,534-lb.
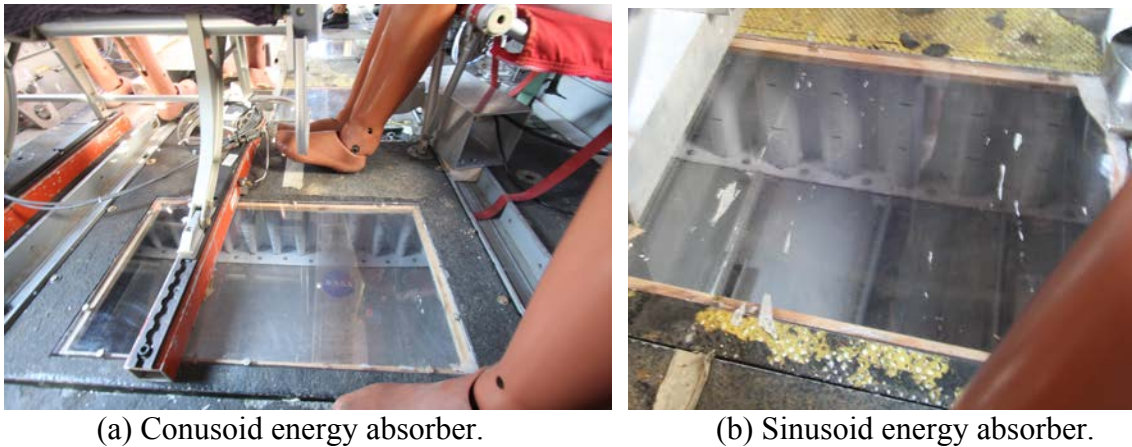
| (a) Conusoid energy absorber. | (b) Sinusoid energy absorber. |

Figure 29. Photographs of the installed energy absorbers.
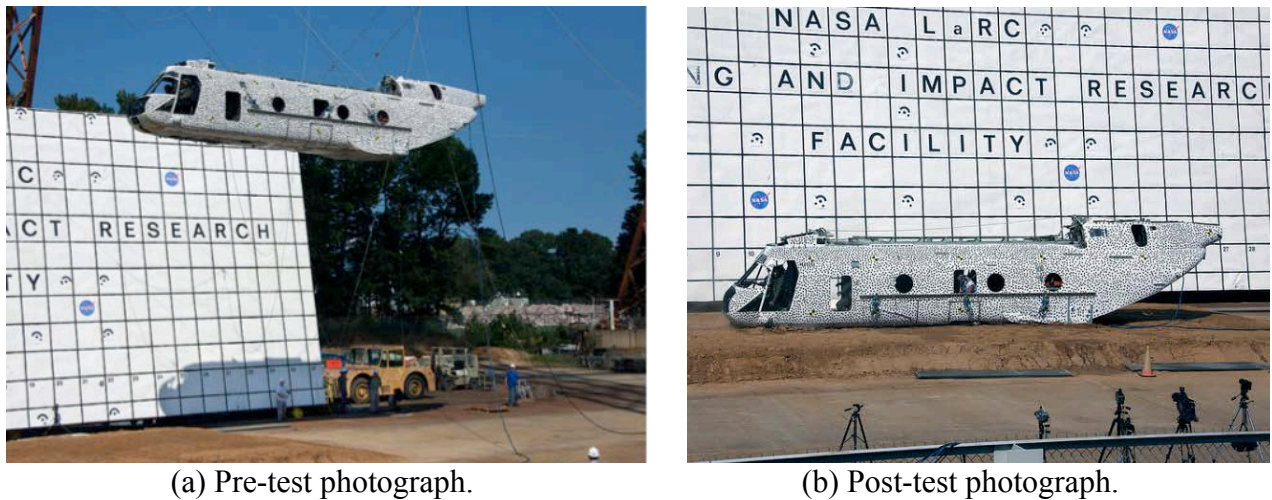
| (a) Pre-test photograph. | (b) Post-test photograph. |

Figure 30. Pre- and post-test photographs of TRACT 2.

The impact surface was a sand/clay mixture. Soil characterization testing [28, 29] was performed both prior to and following the crash test to determine soil density, moisture content, bearing strength, and California Bearing Ratio (CBR). The measured moisture content of the soil was high and it ranged from 9.7 to 16%. Based on post-test measurements, the airframe skidded along the

soil surface approximately 51-in. in the forward direction following initial contact. A post-test photograph is shown in Figure 31 showing the slide out distance from the rear of the airframe.
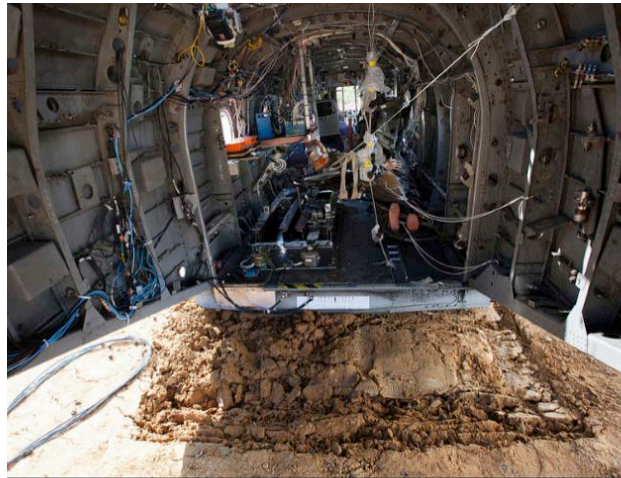

Figure 31. Post-test photograph taken from the rear of the airframe looking forward.

During the impact, the outer belly skin buckled and tore between FS220 and FS286 as it plowed through the soil. The bottom skin skidded approximately 51-in. along the surface of the soil, leaving an 8- to 9-in.-deep divot (maximum depth). As the outer belly skin failed, the floor continued to move forward, which produced shearing in the subfloor beams. The outer skin was torn in several places, while the composite energy absorbing subfloor beams rotated globally under shear loading without significant crushing, as shown in the photograph of Figure 32. The severe outer skin deformation and failure is attributed to wet soil conditions, measured to have a variable moisture content. The crash test was performed a few days following a rainstorm. Even though the soil was covered prior to the test, water was able to penetrate a seam in the tarp. The moist soil produced a higher than anticipated coefficient of friction. For example, TRACT 1 was tested under the same impact conditions onto the same soil and had a slide out of approximately 96-inch [2].

Figure 32. Post-test photograph of the outer belly skin deformation between FS220 and FS286.

Following the impact test, the composite subfloors were removed from the test article. Photographs of the conusoid and the sinusoid foam sandwich energy absorbers are shown in Figures 33(a) and (b), respectively. Note that both photographs show the energy absorbers as they would be positioned facing rearward. The rearward side of both energy absorbers was painted and marked for camera viewing. The conusoid exhibited fracturing on the left and right sides where the energy absorber attached to the fuselage frames. No evidence of crushing or plastic deformation was observed. The sinusoid displayed areas of crush initiation, especially on the bottom left side, as highlighted in the inset photograph of Figure 33(b). Note that a 600-lb. mass was attached to the floor on the left side that straddled the sinusoid energy absorber at FS254. However, the amount of crushing was estimated to be less than 0.5-in.

(a) Post-test photograph of the conusoid energy absorber, rear view looking forward.

(b) Sinusoid energy absorber, rear view looking forward. Inset shows regions of crush initiation.

Figure 33. Post-test photographs of two composite energy absorbers.

6.2 TRACT 2 Finite Element Model

Development of a finite element model of the TRACT 2 test article was completed and predictions of structural impact responses were generated. The airframe model is shown in Figure 34. The model consists of: 218,251 nodes; 13,178 beam elements; 102,413 Belytschko-Tsay shell elements; 119,632 solid elements; 473 parts; 27 material properties; 34 element masses; 19 constrained nodal rigid bodies; 1 initial velocity card; and 1 body load representing gravity. The composite shell elements forming the conusoid and the face sheets of the sinusoid foam sandwich energy absorbers

were represented using Mat 58, with properties listed in Table 1. The foam in the sinusoid sandwich was represented using solid elements assigned Mat 63. Due to early problems with negative volumes in the solid elements representing the sinusoid foam, an erosion card was added to eliminate solid elements once they reached a volumetric strain of 0.9.
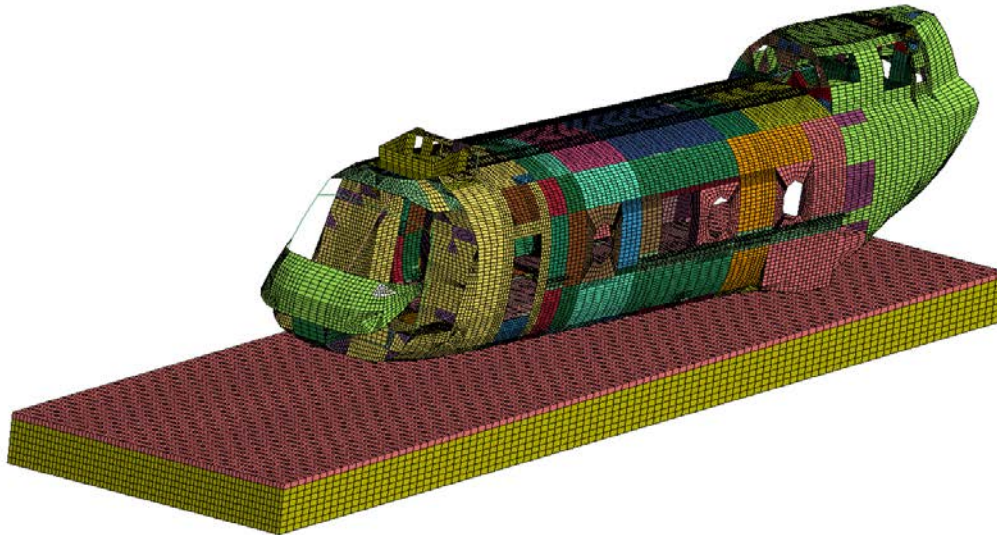

Figure 34. Depiction of the TRACT 2 finite element model.

Finite element models of the sinusoid and conusoid energy absorbers were incorporated into the TRACT 2 model, as shown in Figure 35. These subfloors were located at FS254 and FS286, respectively. Nominal shell element edge length for the conusoid was 0.3-in., compared with a 0.25-in. element edge length for the sinusoid. A detailed structural model of the DLR/ACS-CRC corrugated web subfloor, located at FS220, was not included and was instead modeled as a typical aluminum shear panel.

The soil was represented using solid elements that were assigned Mat 5 (*MAT_SOIL_AND_FOAM) in LS-DYNA®, which is a material model for representing soil and foam [30]. The soil block was 24-in. deep x 148-in. wide x 600-in. long. A coefficient of friction of 0.5 between the airframe and the soil was used in an automatic single surface contact definition. Initially, the soil was represented as a single block with one material model assigned; however, based on the soil characterization results, the model was changed to a layered soil configuration. The top 3-in.-deep layer of soil was represented using Mat 5 with input properties obtained from soil tests conducted on gantry unwashed soil, which were performed for the Orion program [28]. The bottom 21-in. deep layer was also represented using Mat 5 with input properties of sand, whose bearing strength matched in-situ test results conducted prior to and after the TRACT 2 crash test. The bottom and side nodes of the soil model were constrained from motion using a SPC definition in LS-DYNA®.

All nodes forming the helicopter airframe were assigned measured initial conditions of 403.8-in/s (33.65-ft/s) forward and 304.32-in/s (25.36-ft/s) vertical velocities. In addition, the TRACT 2 model was oriented to match the measured impact attitude (2.6° nose-up pitch, 3.5° left-side down roll). Seat/occupant and discrete masses, such as the cargo experiment in the rear of the airframe, were represented using Constrained Nodal Rigid Bodies (CNRBs), as illustrated in Figure 36(a). A 600-lb lumped mass was attached to the left-side floor, centered about FS254, and located above the sinusoid energy absorber, as shown in Figure 36(b).
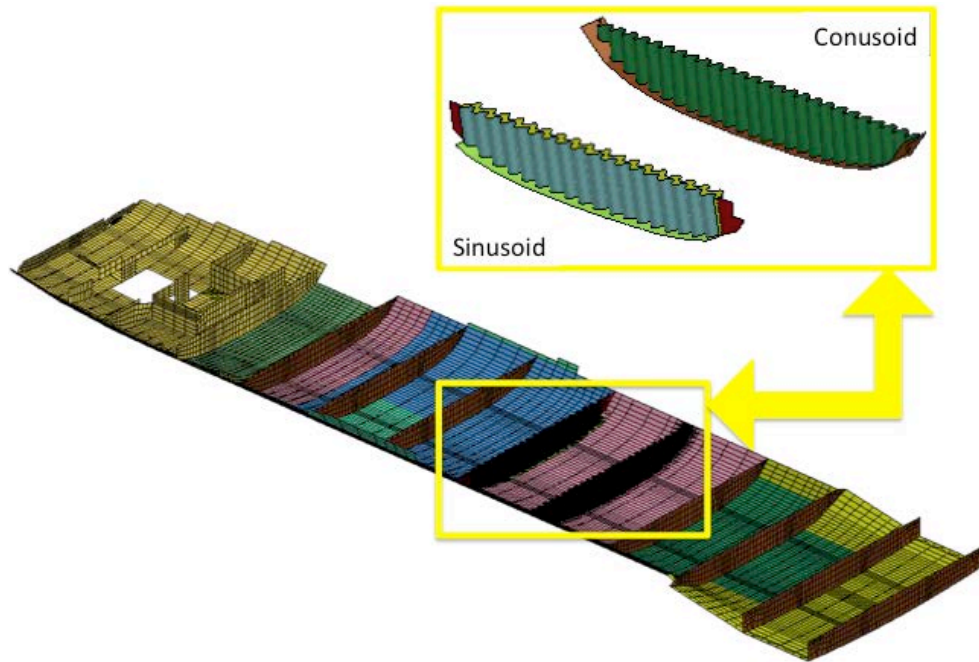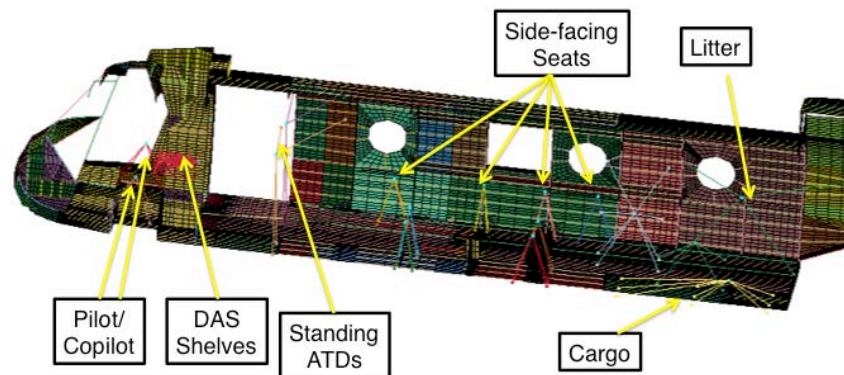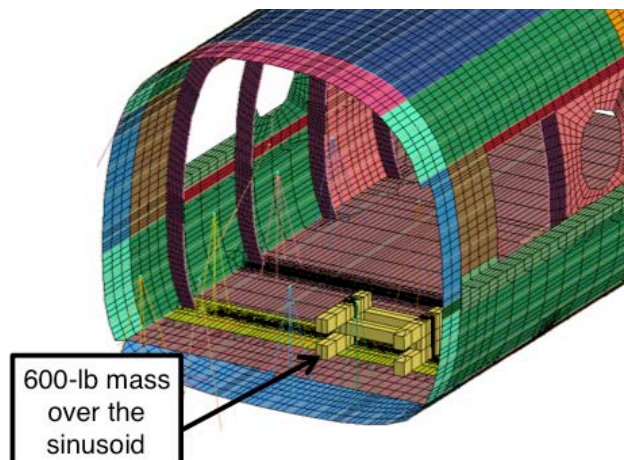
Figure 35. Picture of the outer shell and subfloor sections in the final model.

(a) CNRB locations using in the model.

(b) Location of 600-lb concentrated mass over the sinusoid energy absorber.

Figure 36. Locations of CNRBs and concentrated masses used in the model.

Prior to executing the model, a separate simulation was performed, without the soil, to obtain weight and balance information on the airframe model. Experimental and predicted data are listed in Table 2. In general, the inertial properties of the model compare well with test data. The simulation was executed using LS-DYNA® Version 971 R6.1.1 SMP (double precision) for 0.1-s, which required 74 hours and 35 minutes of CPU time on a Linux-based workstation computer with 8 processors.

Table 2. Comparison of model and test weight and balance data.

	Test	Model
Weight, lb.	10,534	10,534
CG_x, in.	262.8	269.6
CG_y, in.	±0.5	-0.91
CG_z, in.	-10.0	-9.56

Nodal output was requested at locations corresponding to accelerometers mounted on the cabin floor in the test article. The locations of floor-mounted accelerometers, which were attached at the frame/floor junctions on both the left and right sides of the airframe, are illustrated in Figure 37. Test-analysis comparisons were generated at these locations and the experimental and predicted responses were filtered using a 4-pole Butterworth low-pass filter with a cutoff frequency of 60-Hz.
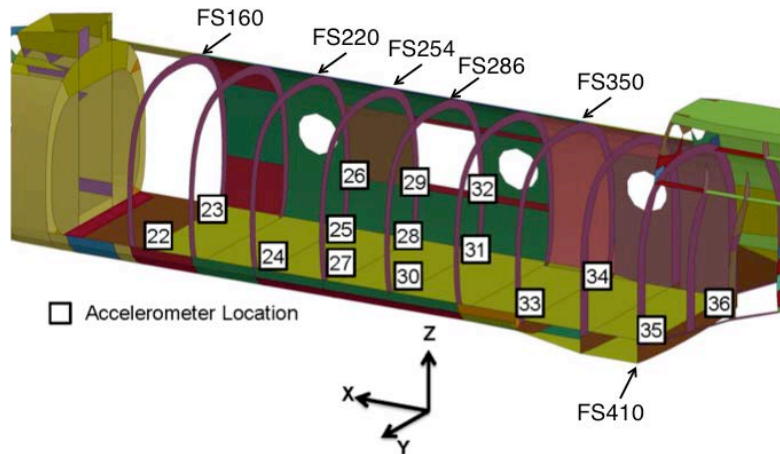

Figure 37. Schematic of fuselage section showing floor-mounted accelerometer locations.

6.3 TRACT 2 Test-Analysis Comparisons

Test and analysis acceleration time histories are shown in Figures 38 through 45 for FS160 through FS410. As noted in Figure 37, these accelerometers were located at the intersection of the floor and the fuselage frames, on the far edges of the floor. In general, the test-analysis comparison results demonstrate a reasonable level of agreement, especially when considering the fact that the actual deformation and failure behavior of the outer skin between FS220 and FS286 was not captured by the model. In the test, the outer belly skin buckled and tore as it plowed through the soil. It is speculated that high shear loading caused the energy absorbing subfloor beams to rotate globally without crushing, as shown in Figure 32, based on the loss of their upper and lower attachments to the floor and outer skin. In order to replicate this response, the energy absorbing subfloor beams in the model would have to be separated from the outer skin and the floor, allowing them the freedom

to rotate in a global manner as their top and bottom constraints failed. However, these modifications to the model were not attempted.
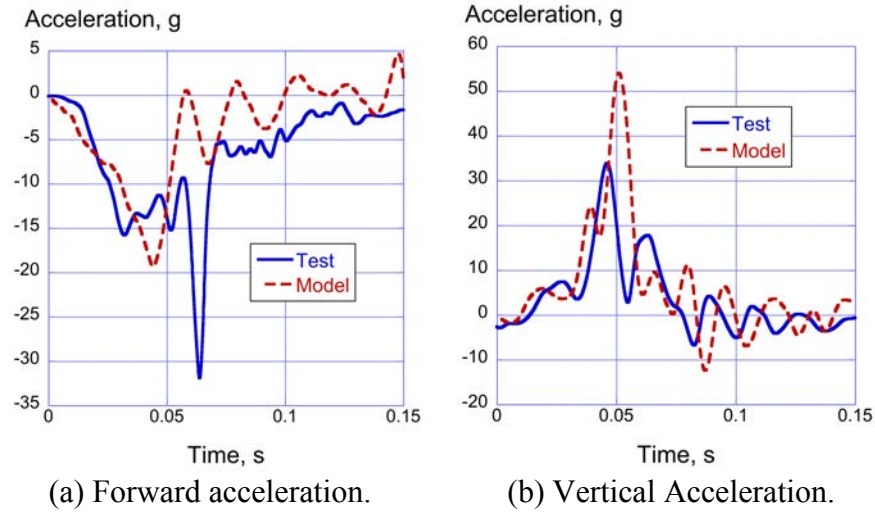

(a) Forward acceleration.   (b) Vertical Acceleration.

Figure 38. Forward and vertical test and analysis acceleration time histories at Left Side FS160.

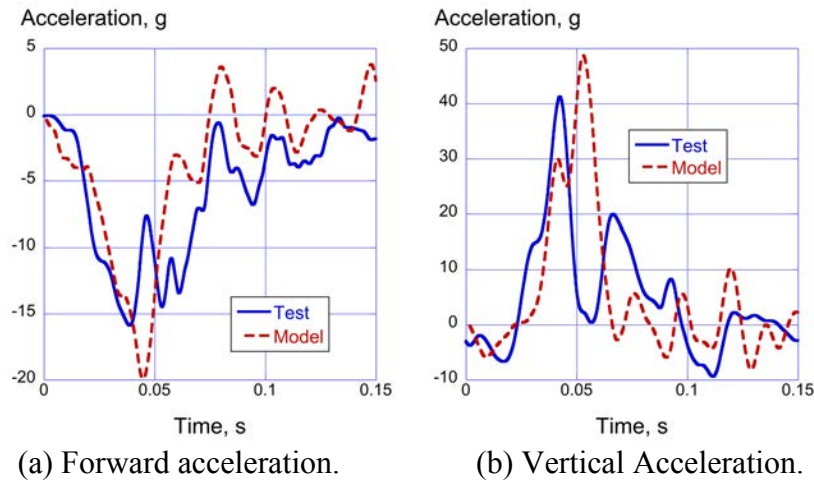(a) Forward acceleration.   (b) Vertical Acceleration.

Figure 39. Forward and vertical test and analysis acceleration time histories at Right Side FS160.

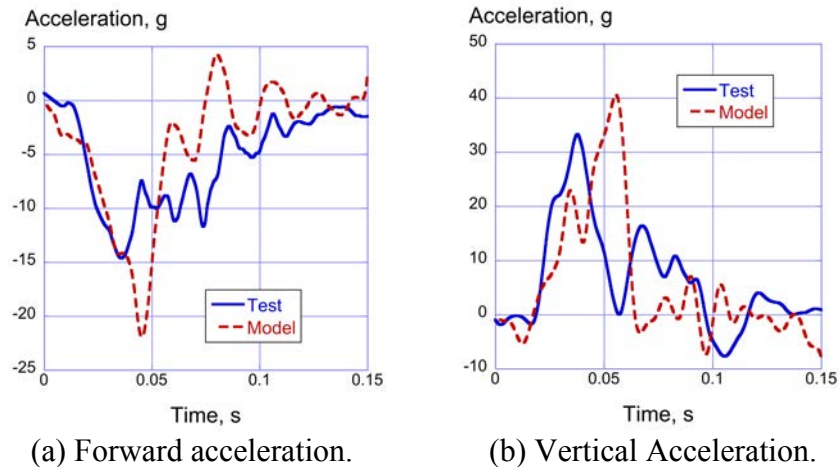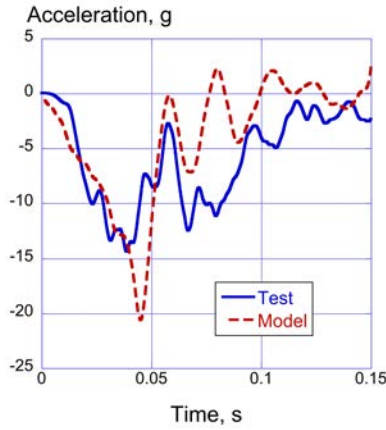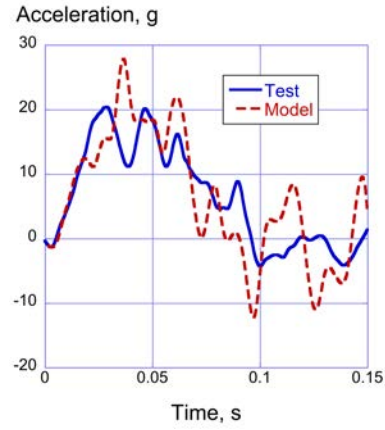(a) Forward acceleration.   (b) Vertical Acceleration.

Figure 40. Forward and vertical test and analysis acceleration time histories at Right Side FS220.
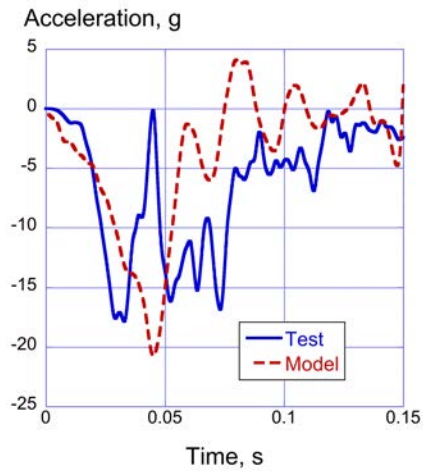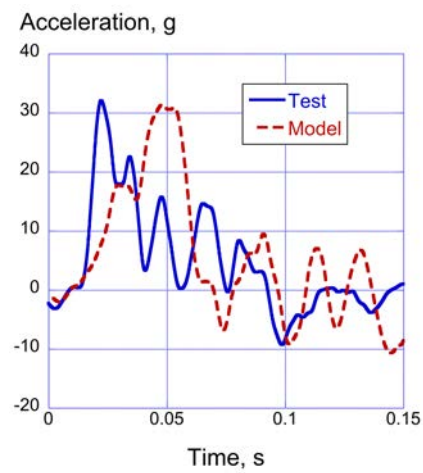
(a) Forward acceleration. (b) Vertical Acceleration.

Figure 41. Forward and vertical test and analysis acceleration time histories at Left Side FS254.

(a) Forward acceleration. (b) Vertical Acceleration.

Figure 42. Forward and vertical test and analysis acceleration time histories at Right Side FS286.

(a) Forward acceleration. (b) Vertical Acceleration.

Figure 43. Forward and vertical test and analysis acceleration time histories at Right Side FS350.

(a) Forward acceleration.   (b) Vertical Acceleration.

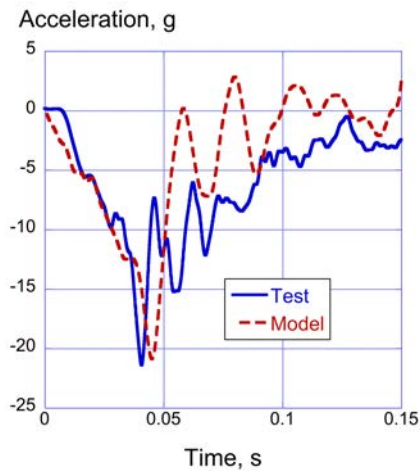Figure 44. Forward and vertical test and analysis acceleration time histories at Left Side FS410.
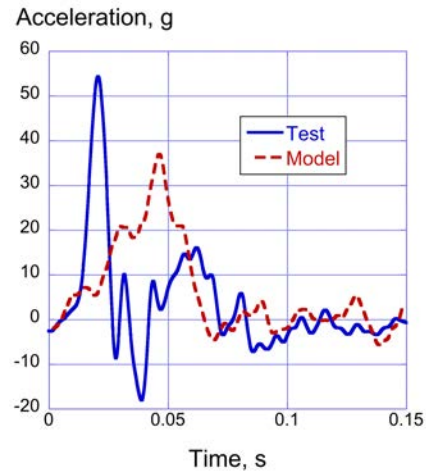

(a) Forward acceleration.   (b) Vertical Acceleration.

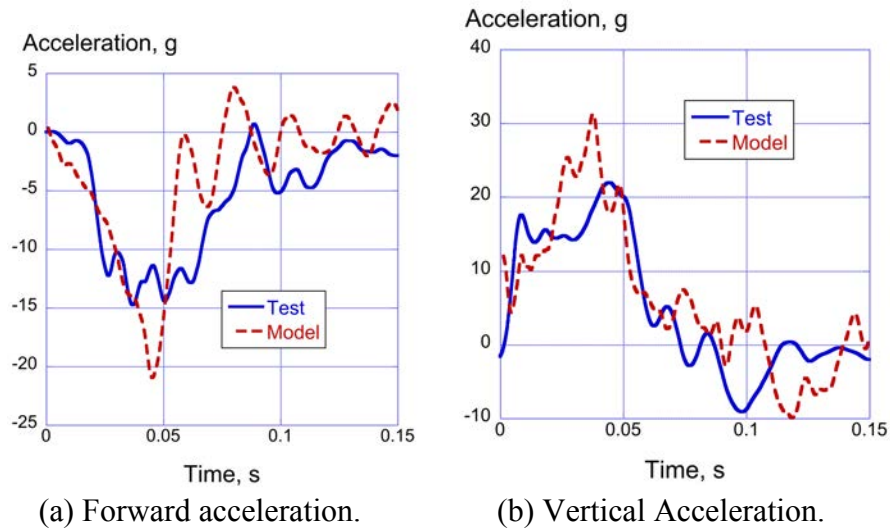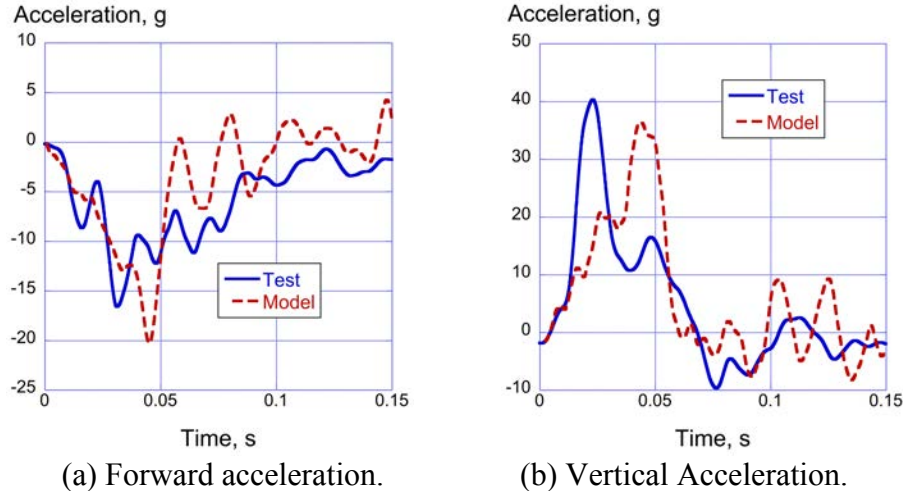Figure 45. Forward and vertical test and analysis acceleration time histories at Right Side FS410.

In the model, the composite subfloor beams behaved in an ideal fashion and exhibited stable crushing. The outer belly skin stayed intact and the energy absorbers crushed between the floor and the outer skin. The conusoid subfloor crushed 48.8% of its original 9.2-in. height, with maximum crushing occurring at 0.06-s. The sinusoid subfloor crushed 42.6% of its original height with maximum crush displacement occurring at 0.06-s. Fringe plots of vertical displacement are shown for the conusoid and sinusoid energy absorbers in Figures 46(a) and (b), respectively, at the time of maximum vertical crush displacement. Of course, these predictions were not realized during the test.

Test-analysis comparison results are shown in Figures 47(a) and (b) for two accelerometers that recorded forward and vertical responses at the base of the double seat located over the conusoid at FS286, near the center of the floor. The experimental and analytical forward acceleration responses are similar and they match the results previously documented in Figures 38(a) through 45(a) for the floor/frame intersection regions. However, the vertical acceleration results vary considerably from previous results. The experimental trace exhibits a dramatic initial peak of 60-g, which is higher

29

than previously shown vertical acceleration traces, followed by a drop in acceleration and a subsequent peak of 22-g. The response is indicative of a sudden shock experienced by the accelerometer, as might be caused by fracture of the sides of the conusoid energy absorber from the fuselage frame at FS286. In contrast, the predicted response exhibits a stable, fairly uniform acceleration of low magnitude (approximately 20-g). This response is indicative of stable crushing of the conusoid, which was predicted, as shown in Figure 46(a).
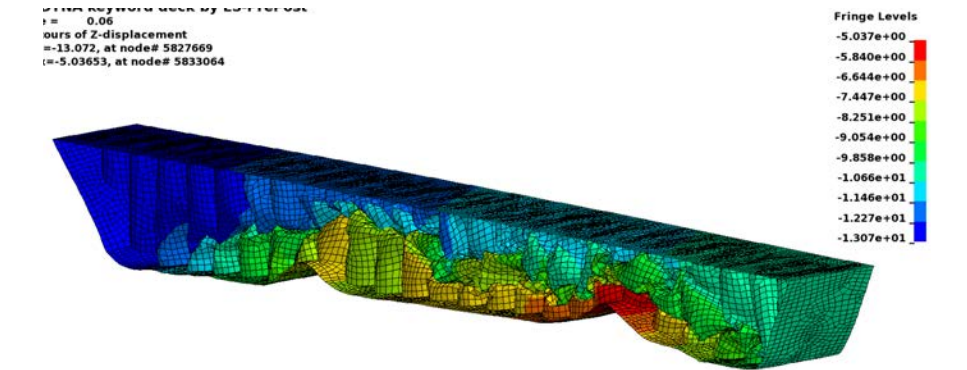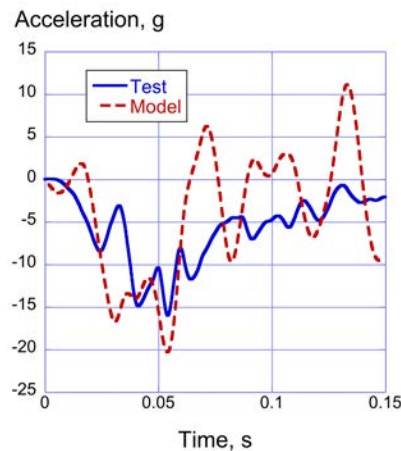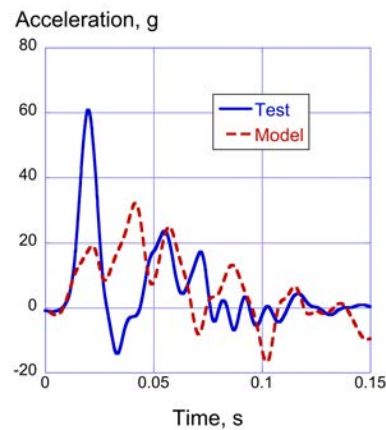

(a) Conusoid energy absorber.
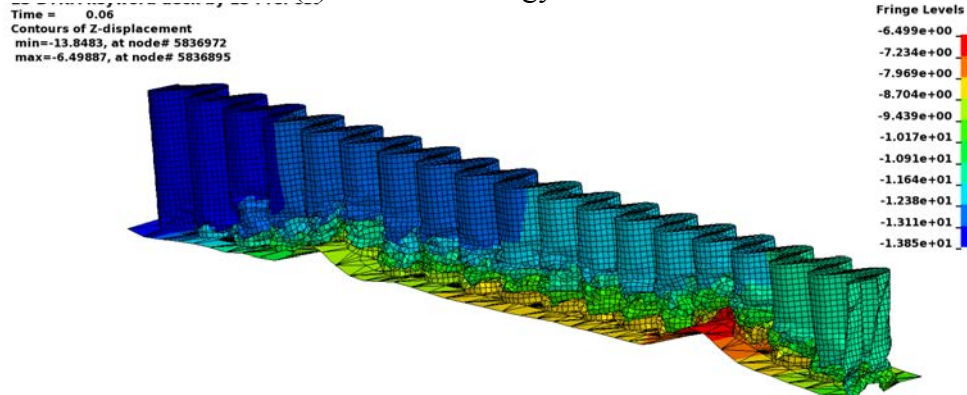
(b) Sinusoid energy absorber.

Figure 46. Depictions of the maximum vertical crush displacements of the conusoid and sinusoid energy absorbers in TRACT 2 at t=0.06-s.

(a) Forward acceleration.   (b) Vertical Acceleration.

Figure 47. Forward and vertical test and analysis acceleration time histories at FS286.

30

A fringe plot of z-displacement is shown in Figure 48(a) of the soil deformation at the time of maximum predicted displacement, which was 5.325-in. Measured maximum displacements were recorded between 8- and 9-in. A photograph of the post-test soil crater is shown in the photograph of Figure 48(b). Note that due to the left roll angle, the soil crater is asymmetric about the centerline. The two images are similar and highlight the asymmetry of the impact event.
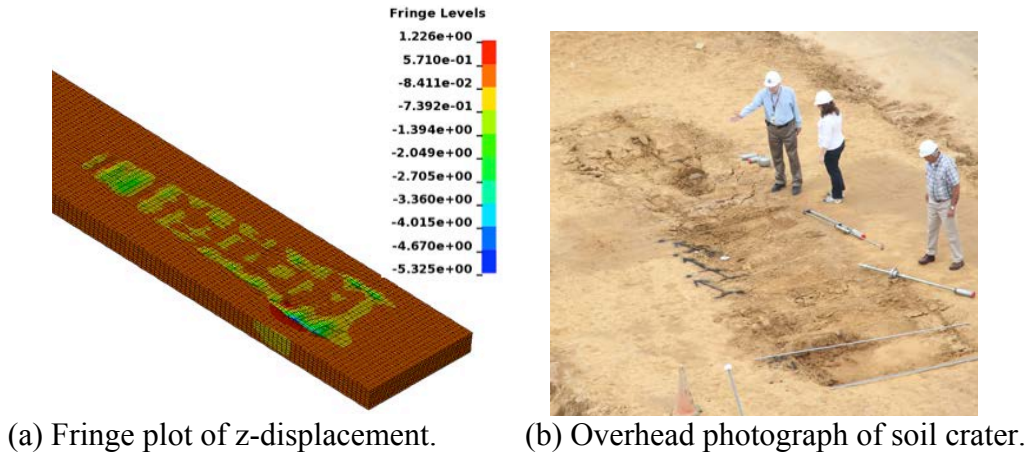
Fringe Levels

1.226e+00
5.710e-01
-8.411e-02
-7.392e-01
-1.394e+00
-2.049e+00
-2.705e+00
-3.360e+00
-4.015e+00
-4.670e+00
-5.325e+00

(a) Fringe plot of z-displacement.   (b) Overhead photograph of soil crater.

Figure 48. Fringe plot of predicted soil deformation and post-test photograph.

7.0 DISCUSSION OF RESULTS

Two objectives of the TRACT 2 project were to assess the capabilities of two novel composite energy absorbers under dynamic impact loading, and to investigate the capabilities of LS-DYNA® to predict the experimental behavior. As stated previously, the design goals for the energy absorbers were to achieve between 25- to 40-g average crush accelerations, to minimize peak crush loads, and to generate relatively long crush stroke limits under dynamic loading conditions, typical of those experienced during the TRACT 1 [2] full-scale crash test. The results of the component tests proved that the energy absorbers met the goal with average crush accelerations of 28-g for the conusoid and 21.8-g for the sinusoid. The lower average crush acceleration for the sinusoid component simply translates into a larger crush stroke than was seen for the conusoid. Test-analysis comparisons are listed in Table 3 for each level of evaluation, component through full-scale testing. Results are presented as percentage differences of average crush acceleration and maximum crush displacements, as appropriate. Note that component test-analysis comparisons agree within 13%.

As shown in Table 3, barrel section comparisons are not as good as for the component tests, mainly due to the fact that some anomalies occurred during the drop test. The conusoid energy absorber bottomed out and two steel bolts interfered with crushing of the sinusoid. However, despite these anomalies, test-analysis comparisons were within 20%, with one exception. For the TRACT 2 test, only average acceleration comparisons are listed in Table 3 for forward (Fwd) and vertical (Vt) acceleration responses generated from floor-mounted accelerometers located between FS160 and FS410. For these comparisons, the pulse durations used to determine average accelerations are listed in parentheses. The selection of the pulse duration for calculating average acceleration was made based on the time at which both test and analysis acceleration traces were approaching zero magnitude. The test-analysis comparisons range from excellent (2.1% agreement for the right-side

vertical acceleration response at FS410) to poor (81.3% agreement for the left-side vertical acceleration response at FS160). For the vertical acceleration comparisons, the level of agreement for six of eight locations was within 18%. It is also useful to note that the measured average forward accelerations were consistent, ranging between 5.8- to 7.8-g, if the one data point obtained from the left-side floor at FS160 is ignored. Finally, it is important to note that, based on soil anomalies during the crash test, a true assessment of conusoid and sinusoid energy absorption behavior as retrofit concepts could not be performed.

Table 3. Test-analysis comparisons.

Test Article Description	Metric	Test	Model	% Difference
Conusoid Component	Avg. Acceleration, g (0.03-s pulse duration)	28.0	28.2	1.43
	Max crush displacement, in.	2.9	2.53	12.8
Sinusoid Component	Avg. Acceleration, g (0.03-s pulse duration)	21.8	22.9	5.0
	Max crush displacement, in.	4.0	3.8	5.0
Barrel Section, 681-lb mass, located above the conusoid	Avg. Acceleration, g (0.06-s pulse)	15	17.5	16.7
	Max crush displacement, in.	8.67	7.8	10.0
Barrel section, 320-lb mass, located above the sinusoid	Avg. Acceleration, g (0.06-s pulse)	14.2	17.0	19.7
	Max crush displacement, in.	6.3	5.24	16.8
TRACT 2, FS160, Lt Fwd	Avg. Accel., g (0.15-s)	3.75	6.8	81.3
TRACT 2, FS160, Lt Vt	Avg. Accel., g (0.078-s)	8.5	11.9	40.0
TRACT 2, FS160, Rt Fwd	Avg. Accel., g (0.133-s)	6.3	4.4	30.2
TRACT 2, FS160, Rt Vt	Avg. Accel., g (0.1-s)	8.7	8.3	4.6
TRACT 2, FS220, Rt Fwd	Avg. Accel., g (0.13-s)	5.9	4.4	25.4
TRACT 2, FS220, Rt Vt	Avg. Accel., g (0.08-s)	13.0	11.7	9.9
TRACT 2, FS254, Lt Fwd	Avg. Accel., g (0.14-s)	6.0	4.1	31.7
TRACT 2, FS254, Lt Vt	Avg. Accel., g (0.1-s)	10.8	10.3	4.3
TRACT 2, FS286, Rt Fwd	Avg. Accel., g (0.15-s)	6.4	4.0	37.5
TRACT 2, FS286, Rt Vt	Avg. Accel., g (0.09-s)	9.0	9.9	10.0
TRACT 2, FS286, Center Fwd	Avg. Accel., g (0.15-s)	5.7	3.9	31.6
TRACT 2, FS286, Center Vt	Avg. Accel., g (0.09-s)	9.7	11.9	22.7
TRACT 2, FS350, Rt Fwd	Avg. Accel., g (0.15-s)	7.1	3.9	45.1
TRACT 2, FS350, Rt Vt	Avg. Accel., g (0.08-s)	8.0	11.6	45.0
TRACT 2, FS410, Lt Fwd	Avg. Accel., (0.15-s)	5.8	3.8	34.5
TRACT 2, FS410, Lt Vt	Avg. Accel., g (0.09-s)	10.7	12.6	17.8
TRACT 2, FS410, Rt Fwd	Avg. Accel., g (0.09-s)	7.8	6.3	19.2
TRACT 2, FS410, Rt Vt	Avg. Accel., g (.07-s)	14.0	14.3	2.1

8.0 CONCLUSIONS

This paper has described the development and multi-level evaluation of two composite energy-absorbing concepts. Both concepts were designed to achieve between 25- to 40-g sustained average crush accelerations, to minimize peak crush loads, and to generate relatively long crush stroke limits

during retrofit onto the second Transport Rotorcraft Airframe Crash Testbed (TRACT 2) full-scale crash test. The first concept, designated the "conusoid," is a conusoidal-shaped design based on alternating right-side-up and up-side down half-cones placed in a repeating pattern. The conusoid combines a simple cone design, with sinusoidal beam geometry to create a structure that utilizes the advantages of both configurations. The conusoid was fabricated of four layers of hybrid graphite-Kevlar® fabric with layers oriented at [+45°/-45°/-45°/+45°]. The second energy absorber, designated the "sinusoid," is a sinusoidal foam sandwich design, which consists of two face sheets oriented at [±45°] fabricated of hybrid graphite-Kevlar® fabric material with a 1.5-in. closed-cell foam core separating the face sheets.

The energy absorbing concepts were evaluated using a multi-level, building-block approach, including both testing and LS-DYNA® simulation. Initially, component specimens were subjected to vertical impact using a 14-ft. drop tower. The components had nominal dimensions of 12-in. in length, 7.5-in. in height and an overall width of 1.5-in. The component tests were used to assess the energy absorption capabilities of the two composite designs. The impact condition for all of the dynamically crushed specimens was approximately 264-in/s (22-ft/s).

Next, subfloor beams of the conusoid and sinusoid foam sandwich configurations were manufactured and retrofitted into a barrel section of a CH-46E helicopter airframe. A vertical drop test of the barrel section was conducted at 297.6-in/s (24.8-ft/s) onto concrete. The objectives of the test were to evaluate: (1) the performance of the two energy absorbers during a full-scale drop test prior to the TRACT 2 test, (2) the fabrication methods for the energy absorbers, (3) the structural integrity of the retrofit, (4) the strength of the polycarbonate floor, and (5) imaging techniques used during the test.

Finally, the two energy absorbers were retrofitted into the subfloor of the TRACT 2 test article, a full-scale CH-46E helicopter airframe. A full-scale crash test was performed onto soil with impact conditions of 403.8-in/s (33.65-ft/s) forward and 304.32-in/s (25.36-ft/s) vertical velocity. The test article contained numerous onboard experiments; however, a major goal of the test was to evaluate the performance of novel composite energy absorbing subfloor designs for improved crashworthiness.

For each multi-level evaluation of the subfloor concepts, test data were used to validate simulations performed using the commercial nonlinear explicit, transient dynamic finite element code, LS-DYNA®. Finite element models were developed to represent dynamic crushing of the component specimens, the vertical impact of the retrofitted barrel section, and the retrofitted TRACT 2 airframe impacting onto soil.

Major findings of this research effort are listed, as follows:
- Both the conusoid and sinusoid foam sandwich concepts proved to be excellent energy absorbers, as demonstrated through component impact tests. The conusoid component exhibited stable folding and crushing up to 38.7% stroke with an average acceleration of 28.0-g, thus meeting the stated design goal. Likewise, the sinusoid component absorbed energy through localized uniform folding of the face sheets and foam crushing. An average acceleration of 21.8-g was recorded for the sinusoid over 50% crush stroke.
- For both components, the LS-DYNA® predictions showed excellent comparison with test data. The LS-DYNA® model of the conusoid predicted an average acceleration of 28.4-g for

the conusoid. Likewise, the average acceleration of the predicted response for the sinusoid component is 22.9-g.

- The barrel section drop test results were complicated by the fact that the conusoid energy absorber bottomed out, allowing the floor to impact the outer skin. In addition, two long bolts used to attach the concentrated mass to the floor over the sinusoid were untrimmed, allowing the bolts to impact the outer skin and deform plastically. Both of these events resulted in large increases in the acceleration responses near the end of the pulses, as measured on the two concentrated masses located over the conusoid and sinusoid energy absorbers. Despite these complications, average accelerations of 15.0- and 14.2-g were measured on the 681-lb and 320-lb concentrated masses located over the conusoid and the sinusoid energy absorbers, respectively.

- During the barrel section impact, the conusoid energy absorber exhibited 58% crush stroke and displayed fracturing and delamination of the hybrid carbon-Kevlar® walls.   The sinusoid foam sandwich energy absorber exhibited 49.3% crush stroke and displayed crushing of the foam core, and fracturing of the face sheets starting from the bottom, curved edge. The sinusoid energy absorber in the barrel section did not exhibit the uniform folding pattern seen in the face sheets of the component specimen.

- LS-DYNA® model predictions for the barrel section drop test were reasonable; however, results indicated that the model was generally too stiff. For example, the predicted maximum crush displacement of the conusoid energy absorber was 7.8-in. and the experimental maximum crush displacement was 8.67-in., a difference of approximately 0.9-in. Likewise, the predicted maximum crush displacement of the sinusoid was 5.24-in. and the experimental maximum crush displacement was 6.3-in., a difference of 1-in.

- Results from the TRACT 2 full-scale crash test were also complicated by anomalies. Moist soil increased the coefficient of friction and reduced the stopping distance of the test article by half, compared with the TRACT 1 test. Due to excessive damage of the outer belly skin, the composite energy absorbers failed to crush and rotated globally as they became separated from the floor and outer skin. Regardless, over 95% of 350-channels of data were collected during the impact test.

- Test-analysis comparisons with data obtained from accelerometers, mainly located at the floor/fuselage frame intersections at FS160 to FS410, were evaluated. These results demonstrated reasonable test-analysis comparisons, despite the fact that the model predicted idealized crush responses for both energy absorbers, which did not match the observed behavior.

- Finally, based on soil anomalies during the crash test, a true assessment of conusoid and sinusoid energy absorption behavior as retrofit concepts could not be performed.

10.0 REFERENCES

1. Jackson, K.E., Fuchs, Y. T., and Kellas, S., "Overview of the NASA Subsonic Rotary Wing Aeronautics Research Program in Rotorcraft Crashworthiness," *Journal of Aerospace Engineering*, Special Issue on Ballistic Impact and Crashworthiness of Aerospace Structures, Volume 22, No. 3, July 2009, pp. 229-239.

2. Annett M.S., Littell J.D., Jackson K.E., Bark L., DeWeese R., McEntire B.J., "Evaluation of the First Transport Rotorcraft Airframe Crash Testbed (TRACT 1) Full-Scale Crash Test," NASA Technical Memorandum, NASA/TM-2014-218543, October 2014.

3. Annett M.S., "Evaluation of the Second Transport Rotorcraft Airframe Crash Testbed (TRACT 2) Full Scale Crash Test," Proceedings of the American Helicopter Society International Annual Forum 71, Virginia Beach, VA, May 3-5, 2015.

4. Kindervater C., Thomson R., Johnson A., David M., Joosten M., Mikulik Z., Mulcahy L., Veldman S., Gunnion A., Jackson A., and Dutton S., "Validation of Crashworthiness Simulation and Design Methods by Testing of a Scaled Composite Helicopter Frame Section," Proceedings of the American Helicopter Society 67th Annual Forum, Virginia Beach, VA, May 3-5, 2011.

5. Billac T., David M., Battley M., Allen T., Thomson R., Kindervater C., Das R., "Validation of Numerical Methods for Multi-terrain Impact Simulations of a Crashworthy Composite Helicopter Subfloor," Proceedings of the American Helicopter Society 70th Annual Forum, Montreal, Quebec, Canada, May 20-22, 2014.

6. Littell J. D., "The Development of a Conical Composite Energy Absorber for use in the Attenuation of Crash/Impact Loads," Proceedings of the American Society for Composites 29th Technical Conference, 16th US-Japan Conference on Composite Materials, September 8-10, University of California San Diego, La Jolla, CA.

7. Hallquist J. Q., "LS-DYNA Keyword User's Manual," Volume I, Version 971, Livermore Software Technology Company, Livermore, CA, August 2006.

8. Hallquist J. Q., "LS-DYNA Keyword User's Manual," Volume II Material Models, Version 971, Livermore Software Technology Company, Livermore, CA, August 2006.

9. Jackson K. E., Morton J., Lavioe A., and Boitnott R.L., "Scaling of Energy Absorbing Composite Plates," *Journal of the AHS*, Vol. 39, No. 1, January 1994, pp. 17-23.

10. Farley G. L., and Jones R.M., "Energy Absorption Capability of Composite Tubes and Beams," NASA Technical Memorandum NASA/TM-101634, September 1998.

11. Farley G. L., "Energy Absorption of Composite Materials*," Journal of Composite Materials*, 17, (5), May 1983, pp. 267-279.

12. Kindervater C. M., "Crash Impact Behavior and Energy Absorbing Capability of Composite Structural Elements," 30th National SAMPE Symposium, March 1985, pp.1191-2101.

13. Bannerman D. C., and Kindervater C. M., "Crashworthiness Investigation of Composite Aircraft Subfloor Beam Sections," Proceedings of the International Conference on Structural Impact and Crashwhiness, J. Morton, editor, Elsevier Applied Science, London, UK, July 1984, pp. 710-722.

14. Hanagud S., Craig J. I., Sriram P., and Zhou W., "Energy Absorption Behavior of Graphite Epoxy Composite Sine Webs," Journal of Composite Materials, 23, (5), May 1989, pp. 448-459.

15. Price J. N., and Hull D., "Axial Crushing of Glass Fibre-Polyester Composite Cones," *Composites Science and Technology*, Volume 28, 1987.

16. Feraboli P., et al. "Design and certification of a composite thin-walled structure for energy absorption," *International Journal of Vehicle Design*, Vol. 44, Nos. 3/4, 2007.

17. Gupta N. K. and Velmurugan, R., "Axial Compression of Empty and Foam Filled Composite Conical Shells," *Journal of Composite Materials*, Vol. 33, No. 6, 1999.

18. Fleming D. C., and Vizzini A. J., "Tapered Geometries for Improved Crashworthiness Under Side Loads," *Journal of the American Helicopter Society*, Vol. 38, 1993.

19. Cronkhite J.D., and Berry V.L., "Crashworthy Airframe Design Concepts, Fabrication and Testing," NASA Contractor Report 3603, NASA Contract NAS1-14890, September 1982.

20. Farley G.L., "Crash Energy Absorbing Composite Sub-Floor Structure," AIAA Paper 86-0944, Proceedings of the 27th AIAA/ASME/ASCE/and AHS Structures, Structural Dynamics, and Materials Conference, San Antonio, TX, May 19-21, 1986.

21. Carden H. D., and Kellas S., "Composite Energy-Absorbing Structure for Aircraft Subfloors," Proceedings of the DOD/NASA/FAA Conference, Hilton Head Island, South Caroline, November 1993.

22. Feraboli P., "Development of a Corrugated Test Specimen for Composite Materials Energy Absorption," *Journal of Composite Materials*, Vol. 42, No. 3, 2008, pp. 229-256.

23. Matzenmiller A., Lubliner J., and Taylor R. L., "A Constitutive Model for Anisotropic Damage in Fiber Composites," *Mechanica of Materials,* Vol. 20, 1995, pp. 125-152.

24. Bark L.W., "Performance Evaluation of Crash-Recording Technologies in a Full-Scale CH-46 Airframe Crash Test," Proceedings of the 71st Annual Forum of the American Helicopter Society, International, Virginia Beach, VA, May 3-5, 2015.

25. Bark L.W., "Testing Mobile Aircrew Restraint Systems in a Full-Scale CH-46 Airframe Crash Test – Exploring the Limits," Proceedings of the 71st Annual Forum of the American Helicopter Society International, Virginia Beach, VA, May 3-5, 2015.

26. Desjardins S.P., and Labun L.C., Selectable Profile Energy Absorber System for Rotorcraft Troop Seats," Proceedings of the 71st Annual Forum of the American Helicopter Society, International, Virginia Beach, VA, May 3-5, 2015.

27. Little E.J., Bakis C.E., Bark L.W., Miller S.W., Yukish M.A., and Smith E.C., "Laboratory and Field Evaluations of Up-Scaled Textile Energy Absorbers for Crashworthy Cargo Restraints," Proceedings of the 71st Annual Forum of the American Helicopter Society, International, Virginia Beach, VA, May 3-5, 2015.

28. Thomas M.A., Chitty D.E., Gildea M.L., and T'Kindt C.M., "Constitutive Soil Properties for Unwashed Sand and Kennedy Space Center," NASA/Contractor Report, NASA/CR-2008-215334, July 2008.

29. Fasanella E. L., Jackson K. E., and Kellas S., "Soft Soil Impact Testing and Simulation of Aerospace Structures," Proceedings of the 10th LS-DYNA Users Conference, Dearborn, MI, June 8-10, 2008.

30. Fasanella E.L., Lyle K.H., Jackson K.E., "Developing Soil Models for Dynamic Impact Simulations," Proceedings of the American Helicopter Society 65th Annual Forum, Grapevine, TX, May 27-29, 2009.

REPORT DOCUMENTATION PAGE		*Form Approved* *OMB No. 0704-0188*

1. REPORT DATE *(DD-MM-YYYY)* 01- 07 - 2015	2. REPORT TYPE Technical Memorandum	3. DATES COVERED *(From - To)*

4. TITLE AND SUBTITLE Multi-Level Experimental and Analytical Evaluation of Two Composite Energy Absorbers	5a. CONTRACT NUMBER
	5b. GRANT NUMBER
	5c. PROGRAM ELEMENT NUMBER
6. AUTHOR(S) Jackson, Karen E.; Littell, Justin D.; Fasanella, Edwin L.; Annett, Martin S.; Seal, Michael D., II	5d. PROJECT NUMBER
	5e. TASK NUMBER
	5f. WORK UNIT NUMBER 380046.02.07.04.01.04

7. PERFORMING ORGANIZATION NAME(S) AND ADDRESS(ES) NASA Langley Research Center Hampton, VA 23681-2199	8. PERFORMING ORGANIZATION REPORT NUMBER L-20579

9. SPONSORING/MONITORING AGENCY NAME(S) AND ADDRESS(ES) National Aeronautics and Space Administration Washington, DC 20546-0001	10. SPONSOR/MONITOR'S ACRONYM(S) NASA
	11. SPONSOR/MONITOR'S REPORT NUMBER(S) NASA-TM-2015-218772

12. DISTRIBUTION/AVAILABILITY STATEMENT
Unclassified - Unlimited
Subject Category 39
Availability: NASA STI Program (757) 864-9658

13. SUPPLEMENTARY NOTES

14. ABSTRACT
Through multi-level testing and simulation performed under the Transport Rotorcraft Airframe Crash Testbed (TRACT) research program. A conical-shaped energy absorber, designated the conusoid, was evaluated that consisted of four layers of hybrid carbon-Kevlar® plain weave fabric oriented at [+45°/-45°/-45°/+45°] with respect to the vertical, or crush, direction. A sinusoidalshaped energy absorber, designated the sinusoid, was developed that consisted of hybrid carbon-Kevlar® plain weave fabric face sheets, two layers for each face sheet oriented at ±45° with respect to the vertical direction and a closed-cell ELFOAM® P200 polyisocyanurate (2.0-lb/ft3) foam core. The design goal for the energy absorbers was to achieve average floor-level accelerations of between 25- and 40-g during the full-scale crash test of a retrofitted CH-46E helicopter airframe, designated TRACT 2. Variations in both designs were assessed through dynamic crush testing of component specimens. Once the designs were finalized, subfloor beams of each configuration were fabricated and retrofitted into a barrel section of a CH-46E helicopter. A vertical drop test of the barrel section was conducted onto concrete to evaluate the performance of the energy absorbers prior to retrofit into TRACT 2. The retrofitted airframe was crash tested under combined forward and vertical velocity conditions onto soil, which is characterized as a sand/clay mixture. Finite element models were developed of all test articles and simulations were performed using LSDYNA ®, a commercial nonlinear explicit transient dynamic finite element code.

15. SUBJECT TERMS

Composite airframe structures; Composite continuum damage; Composite progressive failure model; Element modeling; Explicit transient dynamic finite; Impact testing; LS-DYNA; Mechanics model; Nonlinear

16. SECURITY CLASSIFICATION OF:			17. LIMITATION OF ABSTRACT	18. NUMBER OF PAGES	19a. NAME OF RESPONSIBLE PERSON STI Help Desk (email: help@sti.nasa.gov)
a. REPORT	b. ABSTRACT	c. THIS PAGE			
U	U	U	UU	42	19b. TELEPHONE NUMBER *(Include area code)* (757) 864-9658